Hybrid Stabilization of Closed Orbits for a Class of Underactuated Mechanical Systems

Luiz Navarro, Manfredi Maggiore

***Abstract*— This paper presents a hybrid controller to stabilize a class of closed orbits for mechanical systems with degree of underactuation one. The controller has a hierarchical structure whereby at the low level, a smooth feedback enforces a virtual holonomic constraint in a family, while at the high level a supervisor selects from within the family the constraint to be enforced. To illustrate these ideas, the controller is first used to stabilize oscillations for the acrobot in a manner reminiscent of a child pumping energy on a swing, and then to induce an oscillatory motion in a brachiating robot so as to make its arms bridge the gap between two consecutive handholds.**

***Index Terms*— robot control, nonlinear control systems, motion control**

I. Introduction

Ever since the work of Grizzle and collaborators on bipedal robot locomotion, virtual holonomic constraints (VHCs) have emerged as a tool for motion control in underactuated mechanical systems.

For a robot with degree of underactuation one (one with n configuration variables and $n-1$ actuators), a VHC is a curve in the configuration manifold with the property that with appropriate feedback control, the robot's configuration can be made to converge to and stay on this curve. If a VHC is designed properly, it can be used to solve a variety of interesting problems such as control of pendulum systems [8], [3], bicycles [4], PVTOL aircrafts [6], snake robots [23], brachiating robots [25], [10], and bipedal robots [33].

What makes the VHC framework interesting for motion control is that by shaping the geometry of the VHC curve, one may restrict the behaviour of the robot in a desirable way. For instance, one may design VHCs to execute maneuvers that avoid obstacles in the task space of the robot ([29], [28]).

Another appealing feature of VHCs for robots with degree of underactuation one is that once a VHC has been enforced, the steady-state dynamics are described by a second-order autonomous differential equation, the so-called *reduced dynamics*, whose orbits are easily characterized. The motion planning problem is therefore greatly simplified in the VHC framework ([32], [31], [8]). In particular, the reduced dynamics typically possess a multitude of closed orbits ([21]), each of them representing a repetitive motion of the robot that one may wish to induce via feedback control.

A main challenge in the VHC framework is that all the control degrees-of-freedom are spent enforcing the VHC, and the reduced dynamics are unforced. As such, once a specific closed orbit of the reduced dynamics has been selected, the stabilization of such orbit is a challenging problem. Three main approaches have been used to stabilize closed orbits in the context of VHCs.

The first approach is to design VHCs in such a way that the reduced dynamics possess a stable limit cycle. In the context of bipedal locomotion, Grizzle and collaborators ([33]) have shown that if the VHC curve is suitably designed, the ground impacts can provide an orbit stabilization mechanism. For systems without impacts, the authors in [2] stabilize closed orbits by designing second-order target dynamics possessing a stable limit cycle, and then seek a VHC whose associated reduced dynamics match the target dynamics. This design, however, is not systematic. In [5], [7], the authors develop a procedure for designing VHC curves of sufficiently small length inducing a stable limit cycle. The main drawback in these last two techniques is that one loses control over the geometry of the VHC curve in the configuration manifold and the resulting VHCs may not be useful for solving practical problems.

The second approach ([32], [31]) is to use the VHC only to identify closed orbits of the reduced dynamics. Once a desired orbit has been selected, the VHC is discarded and a controller is designed to locally stabilize the particular orbit. The authors in [32], [31] find the orbit stabilizer through linearization along the orbit. Since this approach does not enforce invariance of the constraint manifold, it does not take full advantage of the VHC geometry to, e.g., avoid obstacles. Furthermore, controllers based on linearization along the orbit can be hard to tune, as they require the numerical solution of a periodic Riccati equation.

The third approach is to dynamically change the VHC to stabilize the desired orbit. In [22], the authors stabilize arbitrary closed orbits of the reduced dynamics by making the constraint dynamic using a controller state as a constraint parameter that is adapted by means of a new control input. This approach, however, relies on the solution of a periodic Riccati equation and it shares with [32], [31] the drawback mentioned in the previous paragraph.

There is a broader literature on stabilization of closed orbits for underactuated mechanical systems which does not rely on VHCs. Of particular note is the recent work of Ortega and

This research was funded by the Natural Sciences and Engineering Research Council of Canada (NSERC).

The authors are with the Department of Electrical and Computer Engineering, University of Toronto, 10 King's College Road, Toronto, ON, M5S3G4, Canada (email: luiz.navarro@mail.utoronto.ca, maggiore@ece.utoronto.ca).

collaborators in [27], [36]. In [27], the authors use the immersion and invariance technique for stabilization of closed orbits, and in [36], they develop the so-called Mexican sombrero energy shaping technique in the context of interconnection and damping assignment for passivity-based stabilization.

Contributions of this paper. The object of this paper is the local asymptotic stabilization of *oscillations*, orbits of the reduced dynamics that resemble the rocking motion of a pendulum (this is made precise in Section II-A). The point of departure is a *nominal* VHC producing reduced dynamics with a target closed orbit that we wish to stabilize. We propose a systematic technique to embed the nominal VHC in a parametric family of VHCs, and a hierarchical controller that locally asymptotically stabilizes the target orbit. At the low level of the hierarchy, a continuous controller enforces a VHC in the family. At the high level, a hybrid supervisor selects the VHC to be stabilized so as to attain two simultaneous objectives: the convergence of the VHC to the nominal VHC and the convergence of the solution to the desired closed orbit. The main result of the paper, Theorem 6.1, shows that the proposed controller ensures asymptotic stability of the target orbit for the closed-loop system provided that the family of constraints enjoys a controllability property.

To illustrate the proposed hybrid controller, we stabilize oscillations for the acrobot in a way resembling the motion of a child on a swing. In a more advanced example, we design a hybrid controller for a five degrees-of-freedom brachiating robot with two arms and a torso inducing an oscillatory motion whereby the arms are made to bridge the gap between two consecutive handholds.

The approach proposed in this paper can be adapted to the stabilization of *rotations*, closed orbits resembling the full revolutions of a pendulum, and this will be presented in following work. Further, while the focus of this paper is on the *local* asymptotic stabilization of closed orbits, our framework lends itself to the development of orbit stabilizers with a guaranteed basin of attraction. This too will be the subject of following work.

Related literature. The idea of using families of VHCs and some kind of supervisor to transition between them is not new in the literature. For instance, it figures prominently in [35, Chapter 7] as a means to regulate the average walking rate in a biped robot. It is also used in the context of gait libraries, e.g., in [26] to create walking gaits with a continuum of desired step lengths to make a biped robot walk on unevenly spaced stepping stones. In these papers, however, the method by which different VHCs in a given family are instantiated in order to achieve a given control objective is quite different than the method presented here because the control objective is different (these papers do not investigate the orbital stabilization of oscillatory motions) and the plant models are different (in these papers, ground impacts affect the robot dynamics, while in this paper there are no ground impacts).

The technique presented in this paper is closest in spirit to the ideas used by Morris and Grizzle in [24] (see also the survey paper [14]), where for bipedal walking robots, a nominal VHC is embedded in a parametric family of VHCs and the parameters are updated at ground impacts to ensure hybrid invariance. In both this paper and [24], the VHC families are indexed via parameters updated at jumps. While jumps in [24] occur due to ground impacts, jumps in this paper are *designed* for orbit stabilization. While in [24] the VHC parameter update is designed to ensure hybrid invariance, in this paper it is the primary orbit stabilization mechanism. In Section XI of this paper, we further compare our main result in Theorem 6.1 to [24, Corollary 11] and [14, Theorem 16].

The lack of ground impacts in this paper means that we cannot assume as given a VHC inducing a stable limit cycle, an assumption common in the literature on bipedal walking. Without ground impacts, a VHC typically induces a continuum of oscillations, all of them stable but not asymptotically stable. The core problem then is to design some mechanism to stabilize a specific oscillation within the aforementioned continuum, and this is the main contribution of this paper.

The idea of using families of VHCs to stabilize an oscillation is also found in [9], where the goal is to enlarge the domain of attraction of an orbit stabilizer for the Furuta pendulum. The authors define a family of orbit stabilizers indexed by a parameter identifying a target orbit in a family, then update this parameter (through switching or dynamically) to gradually transition between the two nominal limit cycles. While in [9] the goal is to enlarge the domain of attraction of a given stable limit cycle, the goal of this paper is to create a stable limit cycle. While the switching mechanism in [9] is based on time, the mechanism presented here is hybrid and based on the system state.

Notation. For $x \in \mathbb{R}$, we denote by $[x]_{2\pi}$ the value of x modulo 2π, and by $[\mathbb{R}]_{2\pi}$ the set of real numbers modulo 2π.

Organization. In Section II we present preliminary notions about virtual constraints and hybrid dynamical systems. In Section III we formulate our control problem. Section IV presents a coordinate transformation using which, in Section V, we propose a systematic technique to embed a nominal VHC in a parametric family of VHCs. Section VI presents the proposed orbit stabilizer and the main stability theorem, Theorem 6.1. In Section VII we explain the controller, and in Section VIII we discuss the steps required to implement it. There we also present a sample family of VHCs. The acrobot example is presented in Section IX, while the brachiating robot is discussed in Section X. The proof of Theorem 6.1 is presented in Section XI. Finally, Section XII presents concluding remarks.

II. Preliminaries

In this paper we study a class of mechanical systems with n degrees of freedom and $n-1$ actuators described by the differential equation

$$D(q)\ddot{q} + C(q,\dot{q})\dot{q} + \nabla_q P(q) = B(q)u, \tag{1}$$

where $q = (q_1, \dots, q_n) \in \mathcal{Q}$ are the configuration variables, $u \in \mathbb{R}^{n-1}$ is the control input, D is the symmetric inertia matrix, assumed to be positive definite, C is the Coriolis matrix, $P : \mathcal{Q} \to \mathbb{R}$ is the potential function and $B : \mathcal{Q} \to \mathbb{R}^{n\times(n-1)}$ is the input matrix, assumed to have full rank $n-1$. We

assume that these functions are C^1 and that the input matrix B has a C^1 left annihilator $B^\perp : \mathcal{Q} \to \mathbb{R}^{1\times n}$ that is nonzero everywhere. We assume that each configuration variable q_i lives either in $\mathbb{R}$ or in $[\mathbb{R}]_{2\pi}$, so that the configuration space $\mathcal{Q}$ is a generalized cylinder. The state space of the mechanical system is the tangent bundle $T\mathcal{Q} := \{(q,\dot{q}) \mid q \in \mathcal{Q}, \dot{q} \in T_q\mathcal{Q}\}$.

A. Virtual Holonomic Constraints

A **virtual holonomic constraint (VHC)** for system (1) is an embedded curve[1] $\mathcal{C} \subset \mathcal{Q}$ that can be rendered invariant via feedback in a precise sense detailed below. We call $\mathcal{C}$ a virtual constraint because the objective is to use the control inputs to constrain the configuration $q \in \mathcal{Q}$ of the system to lie on $\mathcal{C}$.

In order for the configuration $q \in \mathcal{Q}$ to remain on $\mathcal{C}$, it is necessary for the velocity $\dot{q}$ to be tangent to $\mathcal{C}$, so the state $(q,\dot{q}) \in T\mathcal{Q}$ should remain on the tangent bundle of $\mathcal{C}$, $T\mathcal{C} = \{(q,\dot{q}) \in T\mathcal{Q} \mid q \in \mathcal{C}, \dot{q} \in T_q\mathcal{C}\}$. We call the tangent bundle $T\mathcal{C}$ the **constraint manifold** and denote it by $\Gamma \subset T\mathcal{Q}$. The invariance notion alluded to earlier can now be stated precisely. An embedded curve $\mathcal{C}$ is a VHC if the set Γ can be rendered invariant via feedback (i.e., it is controlled invariant).

A sufficient condition for Γ to be controlled invariant is that the control-induced accelerations be transversal to $\mathcal{C}$, i.e., for each $q \in \mathcal{C}$, $T_q\mathcal{C} \oplus \mathrm{Im}(D^{-1}(q)B(q)) = T_q\mathcal{Q}$. A VHC satisfying this transversality condition is said to be a **regular VHC**.

Regular VHCs can be represented in implicit or parametric form. In the **implicit representation**, the VHC is expressed as $h(q) = 0$, where $h : \mathcal{Q} \to \mathbb{R}^{n-1}$ is a smooth map whose differential has full rank $n-1$ on $h^{-1}(0)$. In this representation, we have that $\mathcal{C} = h^{-1}(0)$ and the constraint manifold is given by:

$$\Gamma = \{(q,\dot{q}) \in T\mathcal{Q} \mid h(q) = 0, dh_q\dot{q} = 0\}. \tag{2}$$

Furthermore, it can be seen that the transversality condition for regularity amounts to the property that system (1) with output function $e = h(q)$ has vector relative degree $\{2,\dots,2\}$ on Γ, and Γ is the zero dynamics manifold [1], [17]. In light of this observation, we note that there exists a *unique* feedback on Γ making Γ invariant ([17]) and we can use input-output feedback linearization to obtain a smooth feedback controller rendering the constraint manifold invariant and locally asymptotically stable[2]. This feedback is given by

$$\begin{aligned}\tau(q,\dot{q}) = \left(dh_q D^{-1} B\right)^{-1} \Big[& dh_q D^{-1}\left(C\dot{q} + \nabla_q P\right) - \mathcal{H} \\ & - K_p h - K_d dh_q \dot{q}\Big],\end{aligned} \tag{3}$$

where $\mathcal{H} = [\mathcal{H}_1 \ \dots \ \mathcal{H}_{n-1}]^\top$ with $\mathcal{H}_i = \dot{q}^\top \mathrm{Hess}(h_i)\dot{q}$, and $K_p, K_d \in \mathbb{R}^{(n-1)\times(n-1)}$ are matrix gains chosen to stabilize the $n-1$ dimensional linear system $\ddot{e} + K_d\dot{e} + K_p e = 0$.

In the **parametric representation**, the VHC is given by a relation $q = \sigma(\theta)$, where $\sigma : \Theta \to \mathcal{Q}$ is an embedding with $\Theta = \mathbb{R}$ if the VHC is an open curve, and $\Theta = [\mathbb{R}]_{2\pi}$ if the VHC is a closed curve. In this representation, we have that $\mathcal{C} = \mathrm{Im}(\sigma)$ and the constraint manifold is given by:

$$\Gamma = \{(\sigma(\theta), \sigma'(\theta)\dot{\theta}) \in T\mathcal{Q} \mid (\theta,\dot{\theta}) \in T\Theta\}. \tag{4}$$

The parametric representation is useful because if the VHC is regular and has been made invariant, then the dynamics on the constraint manifold are well defined and can be studied using the diffeomorphism

$$R : T\Theta \to \Gamma, \ (\theta,\dot{\theta}) \mapsto (\sigma(\theta), \sigma'(\theta)\dot{\theta}) \tag{5}$$

to obtain the following reduced order system on $T\Theta$ (see [21], [22], [32], [34]):

$$\ddot{\theta} = \Psi_1(\theta) + \Psi_2(\theta)\dot{\theta}^2, \tag{6}$$

where

$$\begin{aligned}\Psi_1(\theta) &= -\left.\frac{B^\perp \nabla_q P}{B^\perp D\sigma'(\theta)}\right|_{q=\sigma(\theta)} \\ \Psi_2(\theta) &= -\left.\frac{B^\perp D\sigma''(\theta) + B^\perp C\sigma'(\theta)}{B^\perp D\sigma'(\theta)}\right|_{\substack{q=\sigma(\theta)\\ \dot{q}=\sigma'(\theta)}}.\end{aligned} \tag{7}$$

We call system (6) the **reduced dynamics**. Any solution $(q(t),\dot{q}(t))$ of (1) entirely contained in Γ has the form $(q(t),\dot{q}(t)) = R(\theta(t),\dot{\theta}(t))$, where $(\theta(t),\dot{\theta}(t))$ is a solution of the reduced dynamics (6).

If $\Theta = \mathbb{R}$, i.e., the VHC is an open curve, the reduced dynamics are always Lagrangian with Lagrangian $L(\theta,\dot{\theta}) = (1/2)M(\theta)\dot{\theta}^2 - V(\theta)$, where M and V are the **virtual mass** and **virtual potential** functions defined as

$$\begin{aligned}M(\theta) &= \exp\left(-2\int_0^\theta \Psi_2(s)ds\right) \\ V(\theta) &= -\int_0^\theta \Psi_1(s)M(s)ds,\end{aligned} \tag{8}$$

and the **virtual energy**

$$E(\theta,\dot{\theta}) = \frac{1}{2}M(\theta)\dot{\theta}^2 + V(\theta). \tag{9}$$

is an integral of motion of the reduced dynamics (see [19], [21], [32]). When $\Theta = [\mathbb{R}]_{2\pi}$ (i.e., the VHC is a closed curve) then the reduced dynamics are Lagrangian provided that M and V above are 2π-periodic[3].

If the reduced dynamics are Lagrangian, it is straightforward to characterize all closed orbits of the reduced dynamics (see, e.g., [21]). We distinguish two topologically distinct kinds of closed orbits. **Rotations** are images of non-constant periodic solutions of system (6) that can be represented as graphs of functions $\dot{\theta} = \varphi(\theta)$, with $\varphi \neq 0$. These can only occur when $\Theta = [\mathbb{R}]_{2\pi}$. **Oscillations** are images of non-constant periodic solutions of system (6) such that the periodic signal $\theta(t)$ is confined within a strict subset of Θ. See Figure 1 for an illustration of rotations and oscillations. The focus of this paper is on stabilizing oscillations. We also call rotation or oscillation an orbit $\mathcal{O} \subset \Gamma$ of (1) such that $R^{-1}(\mathcal{O})$ is

[1] In other words, a one-dimensional embedded submanifold of the configuration space.

[2] Provided the map $(q,\dot{q}) \mapsto [h(q) \ \ dh_q\dot{q}]^\top$ satisfies mild assumptions [19].

[3] Where θ is treated as a real variable in the computation of the integrals. The topic of the Lagrangian structure of the reduced dynamics is investigated more precisely in [21].

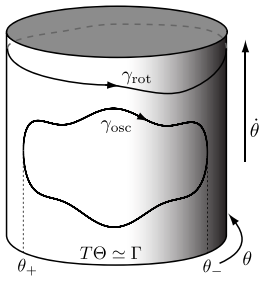

Fig. 1: An illustration of rotations and oscillations for the reduced dynamics in the case when $\Theta = [\mathbb{R}]_{2\pi}$.

a rotation or oscillation of the reduced dynamics (6), where $R : T\Theta \to \Gamma$ is given in (5).

With an oscillation $\mathcal{O} \subset \Gamma$, we associate unique points[4]. $\theta_-, \theta_+ \in \Theta$ such that

$$\begin{aligned} R(\theta_-, 0) \in \mathcal{O}, \;\; \Psi_1(\theta_-) < 0 \\ R(\theta_+, 0) \in \mathcal{O}, \;\; \Psi_1(\theta_+) > 0. \end{aligned} \tag{10}$$

Referring to the reduced dynamics in (6), when $\dot{\theta} = 0$ we have $\ddot{\theta} = \Psi_1(\theta)$ so θ_- identifies the point on γ where $\dot{\theta}$ changes sign from positive to negative. Similarly, θ_+ identifies the point on γ where $\dot{\theta}$ changes sign from negative to positive.

Remark 2.1: In this paper we seek to asymptotically stabilize oscillations. As such, the technique we propose does not require the regularity property to hold over the entire curve $h(q) = 0$. It only needs to hold on a neighborhood of the set $\{q = \sigma(\theta) \mid \theta \in [\theta_+, \theta_-]\}$. △

B. Hybrid Systems

In this paper, we adopt the hybrid dynamical systems framework described in [12], [30]. Accordingly, a **hybrid system** with state $x \in \mathbb{R}^n$ is a 4-tuple $\mathcal{H} = (\mathsf{C}, F, \mathsf{D}, G)$ with associated evolution equations

$$\mathcal{H} \; : \; \begin{cases} x \in \mathsf{C} & \dot{x} = F(x) \\ x \in \mathsf{D} & x^+ = G(x). \end{cases} \tag{11}$$

In the above, $\mathsf{C} \subset \mathbb{R}^n$ and $F : \mathbb{R}^n \to \mathbb{R}^n$ are the flow set and flow map, describing the continuous behaviour of the system, while $\mathsf{D} \subset \mathbb{R}^n$ and $G : \mathbb{R}^n \to \mathbb{R}^n$ are the jump set and jump map, describing the discrete behaviour of the system. If C, D are closed sets and F, G are continuous functions then the hybrid system $\mathcal{H}$ is said to satisfy the **Hybrid Basic Conditions**.

In this paper, hybrid dynamical systems arise from the connection of the continuous plant (1) with a hybrid controller, this latter defined in a manner similar to the above, with an input affecting $F, G, \mathsf{C}, \mathsf{D}$ and an output feeding the plant (see [30]).

A **solution** of the hybrid system (11) is a function $x(t, j)$ whose domain of definition, $\mathrm{dom}(x)$, is a hybrid time domain (see[12] for the definition) and satisfying the following:

- $x(t, j) \in \mathsf{C}$ for all $t \in \operatorname{int} I_j$;
- $\dot{x}(t, j) = F(x(t, j))$ for almost all $t \in I_j$;
- for all $(t, j) \in \mathrm{dom}(x)$, if $(t, j+1) \in \mathrm{dom}(x)$ then $x(t, j) \in \mathsf{D}$ and $x(t, j+1) = G(x(t, j))$,

where $I_j \coloneqq \{t \mid (t, j) \in \mathrm{dom}(x)\}$ and $t \mapsto x(t, j)$ is absolutely continuous on I_j.

A solution x is said to be **complete** if $\mathrm{dom}(x)$ is unbounded. A solution x is said to be **periodic** if there exist $T \geq 0$, $N \in \mathbb{N}$ such that for all $(t, j) \in \mathrm{dom}\, x$ we have $(t + T, j + N) \in \mathrm{dom}(x)$ and $x(t + T, j + N) = x(t, j)$. An **orbit** is a set $\mathcal{O} \subset \mathbb{R}^n$ corresponding to the image of a solution, and a **closed orbit** is the image of a periodic solution.

In this paper we will study stability of closed orbits and sets. Given $\epsilon > 0$ and a set $\Gamma \subset \mathbb{R}^n$, let $\mathbb{B}_\epsilon(\Gamma)$ denote an ϵ-neighborhood of the set Γ, defined as $\mathbb{B}_\epsilon(\Gamma) \coloneqq \{x \in \mathbb{R}^n \mid |x|_\Gamma < \epsilon\}$, where $|x|_\Gamma$ denotes the point-to-set distance of x to the set Γ. Similar to continuous-time systems, we define a set $\Gamma \subset \mathbb{R}^n$ to be **stable for** $\mathcal{H}$ if, for every $\epsilon > 0$ there exists $\delta > 0$ such that any solution x of $\mathcal{H}$ with initial condition $x(0, 0) \in \mathbb{B}_\delta(\Gamma)$ satisfies $x(t, j) \in \mathbb{B}_\epsilon(\Gamma)$ for all $(t, j) \in \mathrm{dom}(x)$.

A set $\Gamma \subset \mathbb{R}^n$ is said to be **pre-attractive for** $\mathcal{H}$ if there exists $\delta > 0$ such that any complete solution x for $\mathcal{H}$ with initial condition $x(0, 0) \in \mathbb{B}_\delta(\Gamma)$ satisfies $|x(t, j)|_\Gamma \to 0$ as $t + j \to \infty$. A set $\Gamma \subset \mathbb{R}^n$ is said to be **pre-asymptotically stable for** $\mathcal{H}$ if it is both stable and pre-attractive.

The **restriction** of a hybrid system $\mathcal{H} = (\mathsf{C}, F, \mathsf{D}, G)$ to a closed set $\mathsf{U} \subset \mathbb{R}^n$ is the hybrid system $\mathcal{H}|_{\mathsf{U}} = (\mathsf{C} \cap \mathsf{U}, F, \mathsf{D} \cap \mathsf{U}, G)$. Given two closed sets $\Gamma_1 \subset \Gamma_2 \subset \mathbb{R}^n$, we say that Γ_1 is pre-asymptotically stable **relative** to Γ_2 if it is pre-asymptotically stable for $\mathcal{H}|_{\Gamma_2}$. The following two results, adapted from [20], can be used to assess pre-asymptotic stability of a set Γ_1 based on its pre-asymptotic stability relative to another set Γ_2.

Lemma 2.2 (Special case of Lemma 2.11 of [20]): For a hybrid system $\mathcal{H} = (\mathsf{C}, F, \mathsf{D}, G)$, if $\Gamma \subset \mathsf{U} \subset \mathbb{R}^n$ are two closed sets such that Γ is compact and $\Gamma \subset \operatorname{int} \mathsf{U}$, then Γ is pre-asymptotically stable for $\mathcal{H}$ if and only if it is pre-asymptotically stable for $\mathcal{H}|_{\mathsf{U}}$.

Theorem 2.3 (Special case of Corollary 4.8 of [20]): For a hybrid system $\mathcal{H}$ satisfying the Hybrid Basic Conditions, consider two sets $\Gamma_1 \subset \Gamma_2 \subset \mathbb{R}^n$ with Γ_1 compact and Γ_2 closed. If:

(i) Γ_1 is pre-asymptotically stable relative to Γ_2, and
(ii) Γ_2 is pre-asymptotically stable for $\mathcal{H}$,

then Γ_1 is pre-asymptotically stable for $\mathcal{H}$.

Theorem 2.3, known as a reduction theorem, will be used to decompose our stability analyses into simpler problems.

Finally, we will need the following Lyapunov theorem for hybrid systems adapted from [30].

Theorem 2.4 (Case 2-d of Theorem 3.19 in [30]): Consider a hybrid system $\mathcal{H} = (\mathsf{C}, F, \mathsf{D}, G)$ on $\mathbb{R}^n$ satisfying the Hybrid Basic Conditions and let $\Gamma \subset \mathbb{R}^n$ be a compact set. Let $W : \mathbb{R}^n \to \mathbb{R}$ be a continuous function that is differentiable on a neighborhood of C and satisfies the following conditions:

(i) $W|_\Gamma = 0$ and $W|_{(\mathsf{C} \cup \mathsf{D} \cup G(\mathsf{D})) \setminus \Gamma} > 0$,

[4]For existence and uniqueness of these points, see equation (9) in [22], as these points are the same as θ^1, θ^2 from [22]

(ii) $L_F W(x) \leq 0$ for all $x \in \mathsf{C}$,
(iii) $W \circ G(x) - W(x) \leq 0$ for all $x \in \mathsf{D}$,
(iv) there is no complete solution $x(t,j)$ of $\mathcal{H}$ satisfying $W(x(t,j)) = W(x(0,0)) > 0$ for all $(t,j) \in \operatorname{dom} x$.

Then Γ is pre-asymptotically stable for $\mathcal{H}$.

III. Problem formulation

Consider the underactuated mechanical system (1), and suppose we have a regular VHC in implicit form, $h(q) = 0$ (henceforth called the **nominal VHC**), inducing Euler-Lagrange reduced dynamics (6) according to the conditions reviewed in Section II-A. Let $\mathcal{O}$ be an oscillation of the constrained dynamics, as defined in Section II-A. The objective of this paper is to design a controller making the solutions of the closed-loop system converge to $\mathcal{O}$ while enforcing a VHC that is closely related to the nominal VHC. We will now make this goal more precise.

As discussed in the introduction, enforcing the VHC $h(q) = 0$ requires using all available control inputs u in (1), which precludes the possibility of stabilizing $\mathcal{O}$. Similarly to what was done in [22], we address this problem by embedding the nominal VHC in a family of VHCs $h^a(q) = 0$, where a is a parameter identifying the VHC within the family and the set of all allowable parameters is denoted by A.

The parameter a is stored as the state of a hybrid controller, $\mathcal{H}_{\text{osc}}$, made up of a continuous part and a discrete part. The continuous part of the controller enforcing the VHC $h^a(q) = 0$ via a feedback $u = \tau^a(q, \dot{q})$ as in (3), while the discrete part updates the parameter a.

The hybrid controller will be designed so that the closed-loop system with state space $T\mathcal{Q} \times \mathsf{A}$ contains a closed orbit

$$\bar{\mathcal{O}} = \{(q, \dot{q}, a) \in \mathsf{C} \mid (q, \dot{q}) \in \mathcal{O},\, \mu(a) = 0\}, \tag{12}$$

where $\mu(a) = 0$ is a condition signifying that the VHC $h^a(q) = 0$ reduces to the nominal VHC $h(q) = 0$, $(q, \dot{q}) \in \mathcal{O}$ implies that the projection of $\bar{\mathcal{O}}$ into $T\mathcal{Q}$ is exactly $\mathcal{O}$, the oscillation we want to stabilize, and the set C is the flow set of the closed-loop system.

In the augmented state space of the closed-loop system, we will define the hybrid constraint manifold

$$\bar{\Gamma} = \{(q, \dot{q}, a) \in \mathsf{C} \mid (q, \dot{q}) \in \Gamma^a\} \tag{13}$$

where Γ^a denotes the constraint manifold associated with the VHC $h^a(q) = 0$. The goal of this paper is to design a hybrid controller $\mathcal{H}_{\text{osc}}$ that simultaneously renders $\bar{\Gamma}$ forward invariant and the orbit $\bar{\mathcal{O}}$ in (12) asymptotically stable.

IV. A useful coordinate system

In order to execute the plan outlined in the previous section, we need a systematic way to embed a given VHC $h(q) = 0$ in a family $\{h^a(q) = 0\}_{a \in \mathsf{A}}$. To this end, we first define a coordinate transformation that simplifies the implicit representation of the VHC. The next result is a direct consequence of the tubular neighborhood theorem ([15]).

A smooth retraction of a manifold M onto a submanifold $N \subset M$ is a smooth map $r : M \to N$ such that $r|_N$ is the identity map on N. Retractions can be thought of as nonlinear generalizations of the notion of projection on vector spaces.

Lemma 4.1: Consider a regular VHC in implicit form $h(q) = 0$, with a regular parameterization $\sigma : \Theta \to h^{-1}(0)$. There exists a neighborhood $\mathcal{W} \subset \mathcal{Q}$ of $h^{-1}(0)$ and a smooth retraction $r : \mathcal{W} \to h^{-1}(0)$ such that letting $\theta^\star := \sigma^{-1} \circ r : \mathcal{W} \to \Theta$, the map $T : \mathcal{W} \to \Theta \times \mathbb{R}^{n-1}$, $q \mapsto (\theta, e) = (\theta^\star(q), h(q))$ is a diffeomorphism onto its image, and in (θ, e) coordinates the VHC is expressed as $e = 0$.

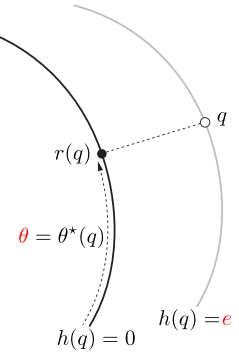

Fig. 2: Geometric interpretation of various objects in Lemma 4.1: the retraction r, the function $\theta^\star(q)$, and the coordinate transformation $(\theta, e) = T(q)$.

Remark 4.2: Given a point $q \in \mathcal{W}$, $\theta^\star(q)$ represents the curve parameter θ such that the point $\sigma(\theta)$ is the projection (not necessarily orthogonal) of q onto the curve $h(q) = 0$ via the retraction r; see Figure 2. The coordinate transformation $(\theta, e) = T(q)$ represents the configuration vector q by means of the parameter θ corresponding to the projection of q onto the curve $h(q) = 0$ and the vector e identifying which level set of h q lies on. In particular, one can take $\theta^\star(q)$ to be the function the maps each q to the curve parameter θ that minimizes the distance between q and $\sigma(\theta)$. For any embedded curve, there exists a neighborhood $\mathcal{W}$ such that for any point $q \in \mathcal{W}$ there is a unique parameter θ that minimizes this distance, and the function $\theta^\star$ defined in this way is smooth (see exercise 6.5 in [18]). △

Example 4.3: Let $h : \mathbb{R}^2 \to \mathbb{R}$ be defined as $h(q) = q_1^2 + q_2^2 - 1$. The zero level set $h^{-1}(0)$ is the unit circle $\mathbb{S}^1$, with parametrization $\sigma : [\mathbb{R}]_{2\pi} \to \mathbb{S}^1$, $\sigma(\theta) = (\cos(\theta), \sin(\theta))$, whose inverse is $\sigma^{-1} : \mathbb{S}^1 \to [\mathbb{R}]_{2\pi}$, $q \mapsto \measuredangle q$, $\measuredangle q$ denoting the angle of q with respect to the q_1 axis, measured counterclockwise. Letting $\mathcal{W} = \mathbb{R}^2 \backslash \{0\}$ and $r : \mathcal{W} \to h^{-1}(0)$ be the orthogonal projection $q \mapsto q/\|q\|$, we get the coordinate transformation $T : \mathcal{W} \to [\mathbb{R}]_{2\pi} \times (-1, \infty)$, $q \mapsto (\sigma^{-1} \circ r(q), h(q)) = (\measuredangle(q/\|q\|), q_1^2 + q_2^2 - 1)$. The inverse is $T^{-1} : [\mathbb{R}]_{2\pi} \times (-1, \infty)$, $(\theta, e) \mapsto \sqrt{e+1}(\cos(\theta), \sin(\theta))$. In this example, $\theta^\star(q) = \measuredangle(q/\|q\|) = \measuredangle q$. △

Example 4.4: For a VHC expressed as the graph of a function, $\operatorname{col}(q_2 \ \dots \ q_n) = \phi(q_1)$, we have the implicit representation $h(q) := \operatorname{col}(q_2 \ \dots \ q_n) - \phi(q_1) = 0$, and the parametrization $q = \sigma(\theta) := \operatorname{col}(\theta, \phi(\theta))$ whose inverse is $\sigma^{-1}(q) = q_1$. We have a globally defined retraction $r : \mathcal{Q} \to h^{-1}(0)$, $q \mapsto \operatorname{col}(q_1, \phi(q_1))$ and map $\theta^\star(q) = \sigma^{-1} \circ r(q) = q_1$. The diffeomorphism T is then given by $T(q) = (q_1, \operatorname{col}(q_2 \ \dots \ q_n) - \phi(q_1))$. △

The function $\theta^\star : \mathcal{W} \to \Theta$ is particularly important in this paper. We define $\dot{\theta}^\star : T\mathcal{W} \to T\Theta$ by $\dot{\theta}^\star(q,\dot{q}) := d\theta^\star_q\,\dot{q}$. Since $\theta^\star$ is defined in a neighborhood of the VHC $h^{-1}(0)$, $\dot{\theta}^\star$ is defined in a neighborhood of the associated constraint manifold Γ. Moreover, for each $(q,\dot{q}) \in \Gamma$, using the diffeomorphism $R : T\Theta \to \Gamma$ in (5), we have by construction that $R(\theta^\star(q), \dot{\theta}^\star(q,\dot{q})) = (q,\dot{q})$.

V. Families of Constraints

Armed with the coordinate transformation of Lemma 4.1, we are ready to systematically embed a given nominal VHC in a family of VHCs. We first present a general way to perform the embedding in question which relies on Lemma 4.1, and then restrict the class of VHC families of interest in this paper.

Definition 5.1: Consider a regular VHC $h(q) = 0$ with a regular parameterization $\sigma : \Theta \to \mathcal{Q}$ and associated coordinate transformation $T : \mathcal{W} \to \Theta \times \mathbb{R}^{n-1}$, $q \mapsto (\theta, e)$, and function $\theta^\star : \mathcal{W} \to \Theta$ given by Lemma 4.1. Let $\{\phi^a : \Theta \to \mathbb{R}^{n-1}\}_{a\in\mathsf{A}}$ be a family of C^2 functions parameterized by $a \in \mathsf{A}$. The corresponding **family of VHCs associated with** $\{\phi^a\}_{a\in\mathsf{A}}$ is a collection of VHCs expressed in (θ, e) coordinates as $e = \phi^a(\theta)$, and in q coordinates represented implicitly as $h^a(q) = 0$ and parametrically as $q = \sigma^a(\theta)$, where

$$h^a(q) := h(q) - \phi^a \circ \theta^\star(q), \tag{14}$$
$$\sigma^a(\theta) := T^{-1}(\theta, \phi^a(\theta^\star(q))). \tag{15}$$

If every constraint in the given family is regular, we say that the family of constraints is regular. △

Having defined the concept of VHC family in general, now we impose structure on the class of VHC families of interest. First, in this paper the parameter a is a triple $a := (\mathsf{d}, \vartheta, \lambda)$ that will be stored as the state of a hybrid controller. The parameter $\mathsf{d} \in \{-1, 1\}$ is a toggle state keeping track of the direction of movement (the symbol d stands for "direction"); -1 indicates backward movement, and 1 indicates forward movement. The parameter $\vartheta \in \Theta$ stores the previous value of $\theta^\star(q)$ at a jump and is used to prevent consecutive jumps. Finally, $\lambda \in \mathbb{R}^{n-1}$ is a parameter vector shaping the geometry of the VHC according to the next definition.

Definition 5.2 (The class $\mathcal{F}$ of function families): Consider a regular VHC $h(q) = 0$ and constants $\delta, r > 0$. Let $\mathsf{B}_r \subset \mathbb{R}^{n-1}$ denote the closed ball of radius r centered at the origin, and define the parameter set

$$\mathsf{A} = \{-1, 1\} \times \Theta \times \mathsf{B}_r. \tag{16}$$

A family of C^2 functions $\{\phi^a : \Theta \to \mathbb{R}^{n-1}\}_{a\in\mathsf{A}}$ is said to be in class $\mathcal{F}$ if the following properties hold:

- **differentiability:** for $\mathsf{d} \in \{-1, 1\}$, the map $(\vartheta, \lambda) \mapsto \phi^{(\mathsf{d},\vartheta,\lambda)}(\theta)$ is C^1;
- **regularity:** for each $a \in \mathsf{A}$ the VHC $h^a(q) = 0$ is regular, where $h^a(q)$ is defined in (14);
- **geometry:** for each $a = (\mathsf{d}, \vartheta, \lambda) \in \mathsf{A}$,

$$\lambda = 0 \text{ implies } \phi^a(\theta) = 0, \tag{17a}$$
$$(d/d\theta)\phi^a(\theta)|_{\theta=\vartheta} = 0, \tag{17b}$$

and $\mathsf{d} = 1$ implies

$$\phi^a(\vartheta) = \lambda \tag{18a}$$
$$|\theta - \vartheta| > \delta \implies \phi^a(\theta) = 0, \tag{18b}$$

while $\mathsf{d} = -1$ implies

$$\phi^a(\vartheta) = 0. \tag{19a}$$
$$|\theta - \vartheta| > \delta \implies \phi^a(\theta) = \lambda. \tag{19b}$$

△

In Section VIII-A we provide a sample family of functions in class $\mathcal{F}$.

The geometric requirement in Definition 5.2 is illustrated in Figure 3 and will be used in what follows to ensure forward invariance of the hybrid constraint manifold $\bar{\Gamma}$ in (13).

Remark 5.3: The regularity requirement in Definition 5.2 is not restrictive when the nominal VHC is a closed curve. Indeed, since the function $(\vartheta, \lambda) \mapsto \phi^{(\mathsf{d},\vartheta,\lambda)}$ is continuous and since $\lambda = 0$ implies $\phi^a(\vartheta) = 0$, then for small λ the relation $h(q) = \phi^a \circ \theta^\star(q)$ defines a regular VHC. △

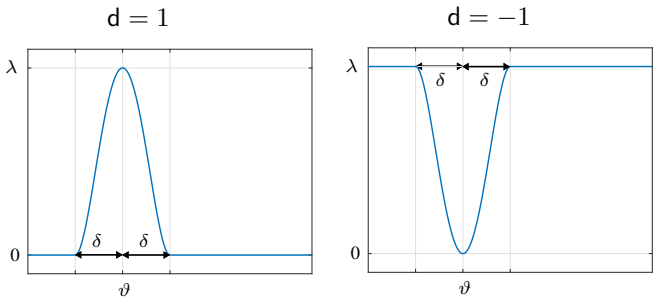

Fig. 3: A sample function ϕ^a meeting the geometric requirement of Definition 5.2 for the case $n = 2$.

VI. Main Result

In this section we present the solution to the orbit stabilization problem formulated in Section III. We begin by reviewing the data of the problem.

Let $h(q) = 0$ be a nominal VHC inducing well-defined virtual mass and potential functions $M(s), V(s)$ defined in (8) and an oscillation $\mathcal{O}$ in the constraint manifold $\Gamma = \{(q,\dot{q}) \in T\mathcal{Q} \mid h(q) = 0, dh_q\dot{q} = 0\}$. This is the target oscillation we wish to stabilize. As discussed in Section II-A, there are unique points $\theta_-, \theta_+ \in \Theta$ associated with $\mathcal{O}$ such that (10) holds. Fix parameters $\delta, r > 0$, with $\delta < |\theta_- - \theta_+|$, and let $\{\phi^a\}_{a\in\mathsf{A}}$ be a family of C^2 functions in class $\mathcal{F}$. Let $h^a(q) = 0$, $h^a = h - \phi^a \circ \theta^\star$, be the corresponding family of regular VHCs. With each member of the VHC family, we associate the constraint manifold

$$\Gamma^a := \{(q,\dot{q}) \mid h^a(q) = 0, (dh^a)_q\,\dot{q} = 0\}.$$

Using the parametrization $q = \sigma^a(\theta)$ given in (15), we get a diffeomorphism

$$R^a : T\Theta \to \Gamma^a,\ R^a(\theta,\dot{\theta}) := (\sigma^a(\theta), (d\sigma^a)_\theta\,\dot{\theta}), \tag{20}$$

using which we get the reduced dynamics

$$\ddot{\theta} = \Psi^a_1(\theta) + \Psi^a_2(\theta)\dot{\theta}^2, \tag{21}$$

in which the functions Ψ_i^a are defined in the same way as Ψ_i in (7) by replacing σ with σ^a. Analogously, we associate with (21) a virtual potential $V^a(s)$, virtual mass $M^a(s)$ and a virtual energy $E^a(s,\dot{s}) = V^a(s) + (1/2)M^a(s)\dot{s}^2$. Replacing h by h^a in (3), we get a stabilizing feedback τ^a for the constraint manifold Γ^a. Finally, the functions $\theta^\star, \dot{\theta}^\star$ arising from Lemma 4.1 enjoy the following property[5] for each $a \in \mathsf{A}$:

$$(\forall (q,\dot{q}) \in \Gamma^a \cap T\mathcal{W})\ R^a(\theta^\star(q), \dot{\theta}^\star(q,\dot{q})) = (q,\dot{q}). \tag{22}$$

Hybrid Controller. Given this data, the proposed hybrid controller with state $a = (\mathsf{d}, \vartheta, \lambda) \in \mathsf{A}$ has the form

$$\mathcal{H}_{\text{osc}} : \begin{cases} (q,\dot{q},a) \in \mathsf{C} & \dot{a} = 0 \\ (q,\dot{q},a) \in \mathsf{D} & a^+ = G_{\text{osc}}(q,\dot{q},a) \\ & u = \tau^a(q,\dot{q}), \end{cases} \tag{23}$$

The stabilizing gain matrices $K_p, K_d \in \mathbb{R}^{(n-1)\times(n-1)}$ from the feedback τ^a are assumed to be symmetric positive definite and independent of a. The flow and jump sets are given by

$$\begin{aligned} \mathsf{C} =& \{(q,\dot{q},a) \mid (q,\dot{q}) \in T\mathcal{W},\ \mathsf{d}\,\dot{\theta}^\star(q,\dot{q}) \geq 0\} \cup \\ & \{(q,\dot{q},a) \mid (q,\dot{q}) \in T\mathcal{W},\ |\theta^\star(q) - \vartheta| \leq \delta\} \\ \mathsf{D} =& \{(q,\dot{q},a) \mid (q,\dot{q}) \in T\mathcal{W},\ \mathsf{d}\,\dot{\theta}^\star(q,\dot{q}) \leq 0\} \cap \\ & \{(q,\dot{q},a) \mid (q,\dot{q}) \in T\mathcal{W},\ |\theta^\star(q) - \vartheta| \geq \delta\} \end{aligned} \tag{24}$$

where $\mathcal{W}$ is the set from Lemma 4.1. The jump map is given by

$$G_{\text{osc}} : \begin{cases} \mathsf{d}^+ = -\mathsf{d} \\ \vartheta^+ = \theta^\star(q) \\ \lambda^+ = \begin{cases} \text{sat}_{\mathsf{B}_r}(v(\theta^\star(q) - \theta_-)) & \mathsf{d} = 1 \\ \lambda & \mathsf{d} = -1. \end{cases} \end{cases} \tag{25}$$

where

$$\text{sat}_{\mathsf{B}_r}(\lambda) = \begin{cases} \lambda & \|\lambda\| \leq r \\ r\frac{\lambda}{\|\lambda\|} & \|\lambda\| \geq r \end{cases} \tag{26}$$

and $v : \Theta \to \mathbb{R}^{n-1}$ is a discrete-time feedback law that we will discuss in a moment. A detailed explanation of this hybrid controller is found in Section VII.

With this controller, the closed-loop system is given by a hybrid system

$$\mathcal{H}_{\text{cl}} = (\mathsf{C}, F_{\text{cl}}, \mathsf{D}, G_{\text{cl}}) \tag{27}$$

with flow and jump sets given by (24) and flow and jump maps given by

$$\begin{aligned} F_{\text{cl}} &= \begin{bmatrix} \dot{q} \\ D^{-1}(q)(B(q)\tau^a(q,\dot{q}) - C(q,\dot{q}) - \nabla P(q)) \\ 0 \end{bmatrix}, \\ G_{\text{cl}} &= \begin{bmatrix} q \\ \dot{q} \\ G_{\text{osc}}(q,\dot{q},a) \end{bmatrix}. \end{aligned} \tag{28}$$

[5]To see why this is the case, note that for each $q \in (h^a)^{-1}(0)$, we have by definition that $h(q) = \phi^a \circ \theta^\star(q)$, and thus $T(q) = (\theta^\star(q), \phi^a \circ \theta^\star(q))$, from which it follows that $q = T^{-1}(\theta^\star(q), \phi^a \circ \theta^\star(q)) = \sigma^a(\theta^\star(q))$. Differentiating this identity we also obtain $\dot{q} = (d\sigma^a)_{\theta^\star(q)}\,\dot{\theta}^\star(q,\dot{q})$, and thus (22) holds.

Given the controller $\mathcal{H}_{\text{osc}}$ in (23), the set

$$\begin{aligned} \bar{\mathcal{O}} = & \{(q,\dot{q},a) \in \mathsf{C} \mid (q,\dot{q}) \in \mathcal{O},\ a = (1,\theta_+,0)\} \cup \\ & \{(q,\dot{q},a) \in \mathsf{C} \mid (q,\dot{q}) \in \mathcal{O},\ a = (-1,\theta_-,0)\} \end{aligned} \tag{29}$$

is a closed orbit of the closed-loop system, whose projection on $T\mathcal{Q}$ is exactly $\mathcal{O}$. Note that this matches the definition given in (12) with

$$\mu(a) = \begin{cases} (\vartheta - \theta_+, \lambda) & \mathsf{d} = 1 \\ (\vartheta - \theta_-, \lambda) & \mathsf{d} = -1. \end{cases} \tag{30}$$

The discrete-time feedback. We show in the proof of Theorem 6.1 below that, if one performs a Poincaré linearization of the closed-loop system $\mathcal{H}_{\text{cl}}$ in (27) along the orbit $\bar{\mathcal{O}}$ in (29), the stability of the resulting Poincaré map is completely determined by the stability of the following scalar discrete-time LTI system with state $z = \theta^\star(q) - \theta_-$:

$$z(k+1) = z(k) + b/(\Psi_1(\theta_-)M(\theta_-))\,v, \tag{31}$$

where

$$\begin{aligned} b = & \frac{\partial}{\partial\lambda}\Big|_{\lambda=0} \Big(V^{(-1,\theta_-,\lambda)}(\theta_+) - V^{(-1,\theta_-,\lambda)}(\theta_-) \\ & + V^{(1,\theta_+,\lambda)}(\theta_-) - V^{(1,\theta_+,\lambda)}(\theta_+) \Big). \end{aligned} \tag{32}$$

We see here the significance of the feedback v appearing in the jump map G_{osc} in (25): it can be used to stabilize the Poincaré map in (31). Accordingly we will assume that b in (32) is not zero (this is a controllability condition) and let $v(z) = v(\theta - \theta_-)$ be a stabilizer for the origin of (31).

The next result shows that, with such a construction, the hybrid controller (23) solves the problem described in Section III.

Theorem 6.1: Consider the construction above, where we fix parameters $\delta, r > 0$ with $\delta < |\theta_- - \theta_+|$, pick a family of functions $\{\phi^a\}_{a\in\mathsf{A}}$ in class $\mathcal{F}$, and define the hybrid controller $\mathcal{H}_{\text{osc}}$ in (23), (24), (25), where the constant vector b in (32) is assumed to be nonzero and the discrete-time feedback $v : \Theta \to \mathbb{R}^{n-1}$ is designed to stabilize the origin of the scalar LTI system (31). Under these assumptions, the closed-loop system $\mathcal{H}_{\text{cl}}$ given in (27) enjoys the following properties:

(a) the hybrid constraint manifold $\bar{\Gamma}$ in (13) is forward invariant;
(b) the lifted orbit $\bar{\mathcal{O}}$ in (29) is asymptotically stable and there are no Zeno solutions in a neighborhood of $\bar{\mathcal{O}}$.

The proof is presented in Section XI.

Remark 6.2: As pointed in Remark 2.1, one can relax the regularity requirement on the nominal VHC so that it only needs to hold on a neighborhood of the set $\{q = \sigma(\theta) \mid \theta \in [\theta_+, \theta_-]\}$. The regularity property in Definition 5.2 can be similarly relaxed and, under such relaxation, the result of Theorem 6.1 will continue to hold on a weaker form. Specifically, property (a) will no longer hold. △

VII. Explanation of Controller

The controller $\mathcal{H}_{\text{osc}}$ has a continuous part, the feedback τ^a enforcing the VHC $h^a(q) = 0$, and a discrete part performing three operations: updating the toggle state d to keep track of forward and backward motion; updating the memory variable

ϑ to store the value of $\theta^\star(q)$ at the last jump; and, updating the vector of parameters λ of the VHC to be instantiated at the next flow.

To illustrate the functioning of the controller, consider the sample orbit in the constraint manifold Γ^a shown in Figure 4. During flow, the controller states $a = (\mathsf{d}, \vartheta, \lambda)$ are kept constant and the VHC $h^a(q) = 0$ is enforced. When $\mathsf{d} = 1$, the system is in forward mode and flows until $\dot\theta^\star(q)$ changes sign from positive to negative. At this point, if $|\theta^\star(q) - \vartheta| > \delta$ then the state has just entered the jump set D and any flow would cause it to leave the flow set C. As such, a jump must happen. At the jump, the plant state is crossing the set[6]

$$\mathsf{P}_{\text{osc}} := \{(q, \dot q, a) \mid \mathsf{d} = 1, \dot\theta^\star = 0\}, \tag{33}$$

and the toggle switch is set to backward mode, i.e $\mathsf{d} = -1$. The state ϑ is updated to store the value of $\theta^\star(q)$ at the jump. This is the apex reached during the forward motion. The state λ is updated according to the feedback v designed to stabilize the scalar discrete-time LTI system (31).

As a result of toggling the variable d, and updating the state ϑ to the current $\theta^\star(q)$, the state after the jump is no longer in D, and therefore the controller jumps only once and cannot do so again until flow drives $\theta^\star(q)$ at least a distance δ away from the last jump. Furthermore, the plant state is now in C and flow is enabled. The controller states are held constant again until the backward motion reaches its apex, i.e., when $\dot\theta^\star$ changes sign from negative to positive.

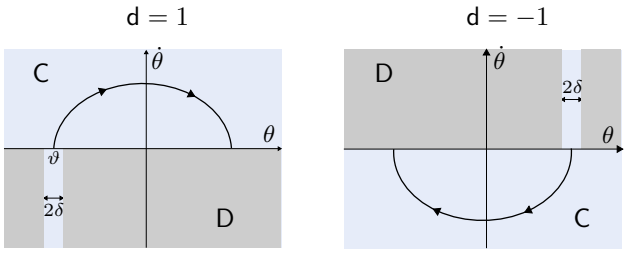

Fig. 4: A sample orbit of the closed-loop system.

We note that the definition of the flow and jump sets relies on two conditions: one condition based on the sign of $\mathsf{d}\,\dot\theta^\star(q, \dot q)$, which forces jumps to happen when the direction of movement changes, and another condition based on the magnitude of $|\theta^\star(q) - \vartheta|$, which prevents multiple consecutive jumps. On the desired orbit $\bar{\mathcal{O}}$, when $\mathsf{d} = 1$, we have that $\vartheta = \theta_+$ and the direction of movement changes when $\theta^\star(q) = \theta_-$. As such, in order for changes in the direction of movement near $\bar{\mathcal{O}}$ to trigger jumps, it is necessary to have $|\theta_+ - \theta_-| > \delta$. If this condition is violated there would be no jumps near $\bar{\mathcal{O}}$ and the stabilization mechanism would fail.

Finally, we note that $\mathsf{C} \cup \mathsf{D} = T\mathcal{W} \times \mathsf{A}$. Since the jump map G_{cl} in (28) does not change $(q, \dot q)$ and does not map a^+ outside of A, we have that the only way maximal solutions of the closed-loop system would not be complete is if the state $(q, \dot q)$ moves outside of $T\mathcal{W}$ during flow. This means that small perturbations due to measurement noise or external disturbances will not cause the controller to stop working.

[6]In the proof of Theorem 6.1 below, this set is a Poincaré section used in the stability analysis.

VIII. Controller Design and Implementation

In this section, we outline the conceptual steps one needs to perform in order to design the hybrid controller $\mathcal{H}_{\text{osc}}$ in (23) and provide an example of a class $\mathcal{F}$ family of functions that can be used in the design.

Step 1. Design a nominal VHC $h(q) = 0$ inducing reduced dynamics (6) with desired properties. In particular, exhibiting closed orbits in the form of oscillations. This problem has been addressed in [29], [28] using the notion of virtual constraint generator.

Step 2. Find a regular parametrization $q = \sigma(\theta)$ of the curve $h(q) = 0$, where $\theta \in \Theta$, and find the function $\theta^\star : \mathcal{W} \to \Theta$ given in Lemma 4.1. Find also the inverse of the diffeomorphism T in that lemma.

The function $\theta^\star$ maps a point $q \in \mathcal{W}$ to the curve parameter $\theta = \theta^\star(q)$ corresponding to the projection of q onto the curve $h(q) = 0$. In typical examples, such as the ones provided in Section IV, the function $\theta^\star$ is easy to find in analytic form. When the curve $h(q) = 0$ has a complex geometric structure, $\theta^\star$ can be found through numerical optimization as $\theta^\star(q) = \arg\min_{\theta\in\Theta} \|q - \sigma(\theta)\|_2$ (see Remark 4.2). Any other vector norm can be used and this optimization can be expressed dynamically as part of the controller (see, e.g., [16, Section 2]).

Step 3. Compute the functions Ψ_1, Ψ_2 in (7) and the virtual mass and virtual potential, M and V, in (8). This latter computation can be performed by numerically integrating the second-order time-varying ODE with state (M, V)

$$\frac{dM}{d\theta} = -2\Psi_2(\theta)M$$
$$\frac{dV}{d\theta} = -\Psi_1(\theta)M,$$

and initial condition $M(0) = 1$ and $V(0) = 0$.

Step 4. Identify a target oscillation of interest, $\mathcal{O}$, by looking at the level sets of the virtual energy function, $E(\theta, \dot\theta)$, in (9) (these give the orbits of the reduced dynamics). Find the associated scalars θ_-, θ_+, the intersections of the closed orbit with the axis $\dot\theta = 0$.

Step 5. Pick parameters $\delta, r > 0$, with $\delta < |\theta_- - \theta_+|$, and choose a family of functions $\{\phi^a : \Theta \to \mathbb{R}^{n-1}\}_{a\in\mathsf{A}}$ in class $\mathcal{F}$, as per Definition 5.2. Below we provide an example of one such family.

Step 6. Check the controllability condition (32). The computation of the vector b in (32) can be performed numerically using finite differences to approximate the derivative with respect to λ at $\lambda = 0$. For instance, we may compute

$$\partial_{\lambda_i}|_{\lambda=0} V^{(1,\theta_-,\lambda)}(\theta_+) \approx \frac{V^{(1,\theta_-,\varepsilon e_i)}(\theta_+) - V(\theta_+)}{\varepsilon}$$

where e_i is the i-th natural basis vector for $\mathbb{R}^{n-1}$ and ε is a small number. The virtual potential $V^{(1,\theta_-,\varepsilon e_i)}(\theta_+)$ is

computed numerically as in Step 3 using now the parametrization $q = \sigma^{(1,\theta_-,\varepsilon e_i)}(\theta)$ given in (15) in which we set $a = (1, \theta_-, \varepsilon e_i)$.

Step 7. Design a feedback $v(z)$ stabilizing the origin of the scalar controllable discrete-time LTI system (31) and use $v(\theta^\star(q) - \theta_-)$ in the jump map G_{osc} in (25). Design constant symmetric positive definite gain matrices K_p, K_d for the feedback τ^a given in (3) (where we use h^a in place of h). This completes the design of the hybrid controller $\mathcal{H}_{\text{osc}}$.

We remark that steps 1-4 are used to set up the problem. The actual control synthesis is elementary, and is covered in steps 5-7.

A. A sample family of functions in class $\mathcal{F}$

It is quite easy to design family of functions meeting the requirements of Definition 5.2. We consider first the case $\Theta = [\mathbb{R}]_{2\pi}$ (i.e., when the nominal constraint is a closed curve in $\mathcal{Q}$). Recall from Definition 5.2 that each function $\phi^a : \Theta \to \mathbb{R}^{n-1}$ must be C^2, and satisfy the continuity, regularity and geometric properties. With this in mind, for a choice of $\delta > 0$ we define

$$\bar{\phi}(s, \lambda) := \begin{cases} 0 & \text{if } |s| > \delta \\ \lambda\,(s-\delta)^2(s+\delta)^2/\delta^4 & \text{if } |s| \le \delta. \end{cases} \tag{34}$$

The function $\bar{\phi}$ enjoys these properties: $\bar{\phi}(s, 0) = 0$, $\bar{\phi}(0, \lambda) = \lambda$, and $\partial_s \bar{\phi}\big|_{(0,\lambda)} = 0$. If we shift this function by ϑ along the s axis, then we can satisfy the geometric conditions for the case of $\mathsf{d} = 1$. To perform the shift we define

$$\begin{aligned} \alpha(s, \vartheta) &:= [s - \vartheta + \pi]_{2\pi} - \pi \\ \phi^{(1,\vartheta,\lambda)}([s]_{2\pi}) &:= \bar{\phi}(\alpha(s, \vartheta), \lambda). \end{aligned} \tag{35}$$

With this choice, $\phi^{(1,\vartheta,\lambda)}(\theta)$ satisfies the differentiability and geometric properties in Definition 5.2. For the case of $\mathsf{d} = -1$, $\phi^{(-1,\vartheta,\lambda)}(\theta)$ can be simply defined as

$$\phi^{(-1,\vartheta,\lambda)}(\theta) := \lambda - \phi^{(1,\vartheta,\lambda)}(\theta), \tag{36}$$

which will also satisfy the differentiability and geometric properties. As discussed earlier, the regularity property amounts to an appropriate choice of the set B_r, which is guaranteed to exist and depends on the base constraint.

Finally, if $\Theta = \mathbb{R}$ (i.e., the nominal constraint curve is not closed), we set $\alpha(s, \vartheta) = s - \vartheta$ and define $\phi^{(1,\vartheta,\lambda)}$ and $\phi^{(-1,\vartheta,\lambda)}$ as in (35) and (36).

IX. The acrobot example

In this section we illustrate the ideas of Section VI by stabilizing oscillations for the acrobot model depicted in Figure 5. This is a two degrees-of-freedom robot with one actuator. The configuration variables are $(q_1, q_2) \in [\mathbb{R}]_{2\pi} \times [\mathbb{R}]_{2\pi}$, and the control input is the torque $\tau \in \mathbb{R}$ at the hip joint. The angle q_1 is measured counterclockwise from the vertical axis with $q_1 = 0$ corresponding to the upward configuration. The angle q_2 is measured counterclockwise relative to q_1 with $q_2 = 0$ corresponding to the fully extended configuration. Modeling each link as a point-mass m at the end of a massless rod

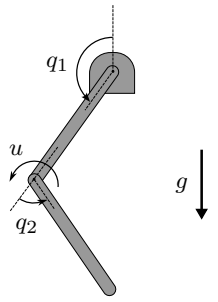

Fig. 5: The acrobot.

of length l, the mathematical model of the acrobot has the form (1) with

$$\begin{aligned} D(q) &= ml^2 \begin{bmatrix} 2\cos q_2 + 3 & \cos q_2 + 1 \\ \cos q_2 + 1 & 1 \end{bmatrix} \\ C(q, \dot{q}) &= ml^2 \begin{bmatrix} -\dot{q}_2 \sin q_2 & -(\dot{q}_1 + \dot{q}_2)\sin q_2 \\ \dot{q}_1 \sin q_2 & 0 \end{bmatrix} \\ P(q) &= 2mgl\cos q_1 + mgl\cos(q_1 + q_2). \end{aligned} \tag{37}$$

We assume that $m = 1\,\text{Kg}$ and $l = 1\,\text{m}$.

The acrobot can be viewed as a simplified model of a child on a swing if we think of the first link as representing the swing plus torso and thighs, and of the second link as representing the lower legs. Following this analogy, the nominal VHC corresponding to the lower legs being extended perpendicular to the torso is $h(q) := q_2 - \pi/2 = 0$, and the corresponding parametrization is $q = \sigma(\theta) = [\theta\ \pi/2]^\top$. One may check that this VHC is regular as $dh_q D^{-1}(q)B \neq 0$.

Since the constraint can be viewed as the graph of a function of q_1, the function $\theta^\star(q)$ in Lemma 4.1 is given by (see Example 4.4) $\theta^\star(q) = q_1$. The diffeomorphism T is defined on the whole $\mathcal{Q}$ and given by $T(q) = (q_1, q_2 - \pi/2)$. Using the parametrization $q = \sigma(\theta)$ just given, we get the reduced dynamics

$$\ddot{\theta} = g(\cos(\theta) + 2\sin(\theta))/3,$$

whose phase portrait is shown in Figure 6. The virtual mass and potential functions are

$$M(\theta) = 1, V(\theta) = -g(\sin(\theta) - 2\cos(\theta) + 2)/3.$$

All the orbits in the shaded region of Figure 6 correspond to oscillations in the nominal constraint. We select the target oscillation with $\theta_- = [1.3\pi]_{2\pi}$ and $\theta_+ = [0.4048\pi]_{2\pi}$ (note that $V(\theta_-) = V(\theta_+)$).

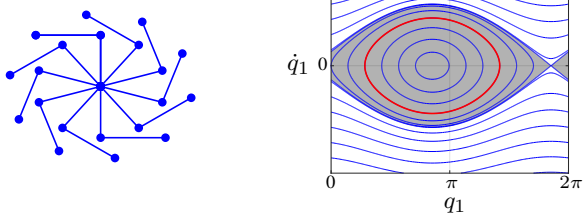

Fig. 6: Nominal constraint and phase portrait of the reduced dynamics.

Using the class $\mathcal{F}$ family of functions defined in Section VIII-A with $\delta = 0.1\pi$ and $r = 1.5$, we numerically compute the constant vector b (in this case a 1×1 vector) in (32) using the finite difference approximation reviewed in Section VIII and obtain $b = 1.84$.

We next design the stabilizing feedback $v(z) = -((\Psi_1(\theta_-)M(\theta_-))/b)\, z$ placing the eigenvalue of system (31) at 0. Finally, we choose gains $K_p = 100, K_d = 20$ for the controller τ^a in (23), placing the poles of the system $\ddot{e} + K_d\dot{e} + K_p = 0$ at -10. The control design is complete.

We simulate the acrobot with controller (23) for 10 oscillations and with initial condition $q(0) = [0.6\pi\, 0.5\pi]^\top$, $\dot{q}(0) = [0\, 0]^\top$ and $(\vartheta, \lambda) = (0, 0)$. The evolution of the acrobot configuration and its reduced dynamics are shown in Figures 7 and 8 and a snapshot representation of the different motions in this simulation is shown in Figure 9.

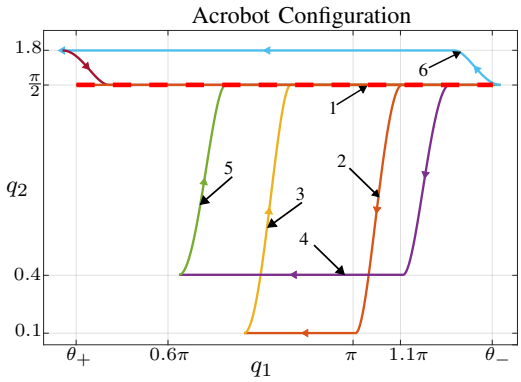

Fig. 7: Projection of the simulated orbit on the configuration space, illustrating the different VHCs being used. The numbers indicate the number of swings of the acrobot around the pivot. The dashed red curve is the nominal VHC.

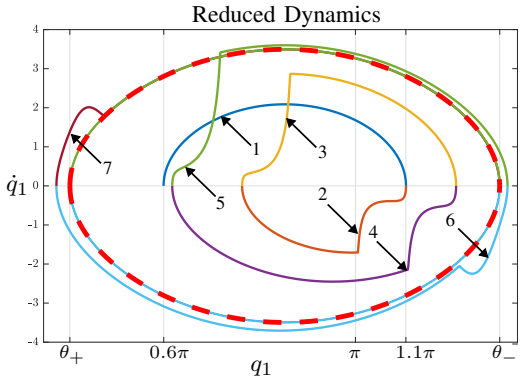

Fig. 8: Projection of the simulated orbit on the constraint manifold. The numbers indicate the number of swings of the acrobot around the pivot. The dashed curve shows the desired orbit.

From the first segment in the configuration plot we see that the acrobot configuration starts in the nominal VHC and remains in it until the direction of movement changes. The same segment on the reduced dynamics plot shows us that, in this first motion, the acrobot is moving in the forward direction, with θ starting on 0.6π and increasing to 1.1π where

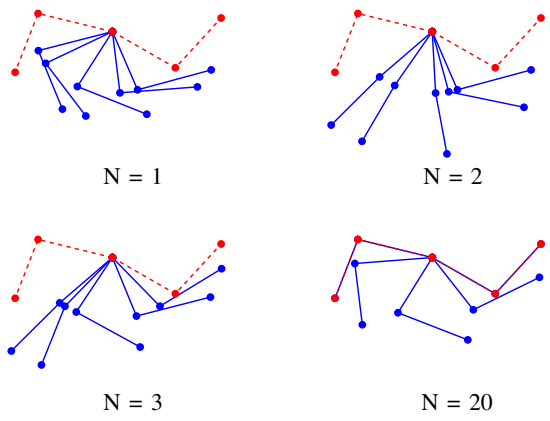

Fig. 9: Illustration of different motions in the acrobot. Each plot corresponds to a single phase of the motion and consists of snapshots of the acrobot configuration taken at equally spaced time intervals. The dashed red lines indicate the desired amplitude of oscillation.

the direction of movement changes. At this point, the discrete part of the controller kicks in and selects new constraint parameters determining the behaviour in the next segment of the motion.

In the second segment of the motion, we can see on the configuration plot that the angle q_2 decreases from 0.5π to roughly 0.1 as the swing moves backwards from 1.1π until the point where the direction of movement changes. This corresponds to the child bending the legs down as the swing moves backwards and it is represented in the $N = 2$ image in Figure 9. We notice in the reduced dynamics plot that this segment has a smaller amplitude compared to the first one. Once the velocity reaches zero the controller chooses a new set of parameters and we start the third segment of the motion. We see in the configuration plot that q_2 quickly returns to 0.5π as q_1 increases, and from the reduced dynamics we see that the amplitude of the motion is larger compared to the first segment. This corresponds to the child extending his legs as the swing moves forward and is represented in the $N = 3$ image in Figure 9.

This process is then repeated once more in segments 4 and 5 where a smaller value of λ is chosen and a larger amplitude of motion is achieved. After a small overshoot, the system reaches the desired orbit in the nominal VHC and stays in it until the end of the simulation.

X. The Brachiating Robot Example

In this section, we use our proposed technique to control the five degrees-of-freedom brachiating robot depicted in Figure 10. The robot consists of a torso and two arms with articulated elbows. The goal is to stabilize a motion where the robot swings with sufficient amplitude to bridge the gap between handholds. Every joint is actuated except for the one connecting the robot to the current handhold.

This configuration is similar to the five degrees-of-freedom model used in [13]. We model the links as point-masses of 1kg attached by massless rods of length 1m. The mathematical model of the robot has the form (1). A MATLAB script

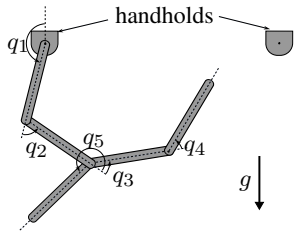

Fig. 10: The brachiating robot.

that symbolically computes these dynamics can be found on `https://github.com/lhanavrro/brachiation`.

Control of brachiating motions is usually a complex task involving multiple stages such as swinging up to reach a handhold, releasing and grasping handholds and controlling the motion between handholds, which may include a flight phase where the robot is not grasping any handhold. It requires consideration about the types and distribution of handholds and geometric constraints from the environment. For a more comprehensive treatment of this problem see [11], [13], [10].

In the case where the brachiating robot is continuously swinging forward and switching handholds, its motion is analogous to that of an upside-down walking robot, with the switching of handholds being similar to a foot's impact with the ground. However, in the case where the brachiating robot does not have enough energy to reach the next handhold, a different type of motion needs to be considered which is significantly different from anything seen in walking robots. This motion consists of a sequence of oscillations of increasing amplitude designed to inject enough energy to the robot so that it can reach the next handhold. In this example we will show one way the technique developed in this paper can be used to implement such motion.

Inspired by the underhand motion in Figure 10 of [11] and the ricochetal motion in Figure 14 of [13], we will attempt to stabilize the motion illustrated in Figure 11, which can be encoded as a VHC given in parametric form as $q = \sigma(\theta)$ with

$$\sigma(\theta) := \begin{bmatrix} \theta & (\theta - \pi) & 2\theta & (\theta - \pi) & (2\pi - 2\theta) \end{bmatrix}^\top \tag{38}$$

where θ ranges from $\frac{5}{6}\pi$ to $\frac{7}{6}\pi$.

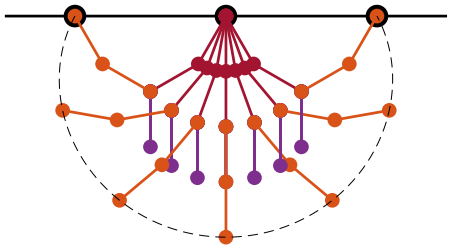

Fig. 11: Proposed motion for the brachiation robot.

Since the motion of interest has θ constrained to the interval $[\frac{5}{6}\pi, \frac{7}{6}\pi]$ we only need to check regularity of the VHC in a neighborhood of this interval. In fact, we have that

$$\begin{aligned} B^\perp D(\sigma(\theta))\sigma'(\theta) = 29\cos(\theta) - 20\cos(\theta)^2 \\ - 68\cos(\theta)^3 + 48\cos(\theta)^4 + 18 \geq 7. \end{aligned} \tag{39}$$

Since there are no zeros in the interval of interest, we have that the proposed VHC is regular.

Using (8), we compute the virtual mass and potential for the parametric VHC in (38), from which we obtain the phase portrait of the reduced dynamics shown in Figure 12. The orbit highlighted in red is the orbit we wish to stabilize, with the associated values of θ_+ and θ_- given by $\theta_+ = [(5/6)\pi]_{2\pi}$ and $\theta_- = [(7/6)\pi]_{2\pi}$.

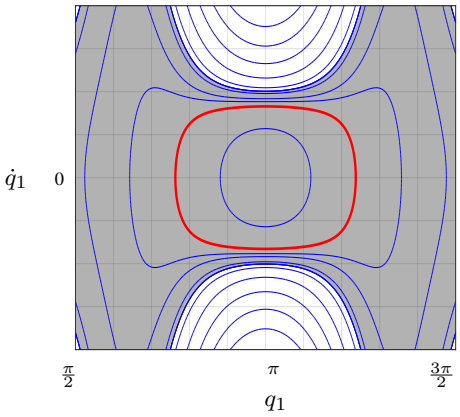

Fig. 12: Reduced dynamics on the proposed VHC.

Similar to the acrobot example, we note that the given VHCs are graphs of functions of q_1 and therefore we can take $\theta^\star(q) = q_1$ and the diffeomorphisms $T(q)$ for each VHC can be directly obtained from (38).

With the class $\mathcal{F}$ family of functions defined in Section VIII-A with $\delta = 0.05\pi$ and $r = 1$, we numerically compute the constant vector b in (32) using the finite difference approximation reviewed in Section VIII and obtain

$$b = \begin{bmatrix} 0.1060 & -0.2434 & -0.1398 & 0.0784 \end{bmatrix}. \tag{40}$$

Next, we design the feedback v described in Section VI. Similar to our approach in the acrobot, we will choose a linear state feedback placing the eigenvalue of system (31) at 0. Given a vector $L \in \mathbb{R}^{n-1}$, the feedback

$$v(z) = -\frac{\Psi_1(\theta_-)M(\theta_-)}{bL} Lz \tag{41}$$

places the eigenvalue of system (31) at 0. It is worth noting that any vector L works for this, as long as $bL \neq 0$. In particular, the vector L can be chosen to satisfy some additional constraints of the problem. In this example we choose $L = \begin{bmatrix} 0 & 2 & 1 & 0 \end{bmatrix}^\top$, ensuring the discrete-time controller acting at jumps will only affect the motion of the swinging arm while keeping the motion of the torso and the grasping arm unchanged.

Finally, we choose gains $K_p = 100I_4, K_d = 20I_4$ for the controller τ^a in (23), where $I_4 \in \mathbb{R}^{4\times4}$ denotes the identity matrix. This places the poles of the system $\ddot{e} + K_d\dot{e} + K_p = 0$ at -10, making the hybrid constraint manifold asymptotically stable. The control design is complete.

We simulate the system with this controller using an initial condition with $q = \sigma(0.9\pi)$, $\dot{q} = 0$, $\mathsf{d} = 1$, $\vartheta = 0$, $\lambda = 0$. The results, shown in Figures 13 and 14, are similar to the

ones obtained for the acrobot example. The solutions of the closed-loop system converge to a small neighborhood of the target orbit after seven jumps.

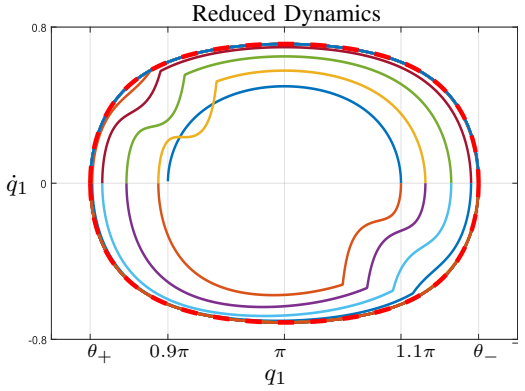

Fig. 13: Projection of the simulated orbit on the constraint manifold. The dashed curve shows the desired orbit.

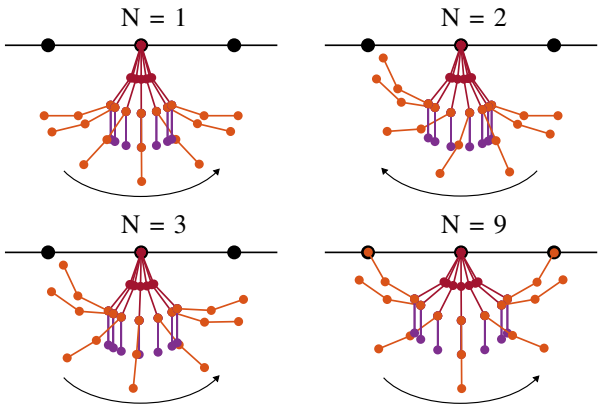

Fig. 14: Illustration of different motions in the brachiation. Each plot corresponds to a single phase of the motion and consists of snapshots of the brachiating robot configuration taken at equally spaced time intervals.

XI. Proof of Theorem 6.1

The proof of Theorem 6.1 has three parts, roughly summarized as follows. First, we show that the hybrid constraint manifold $\bar{\Gamma}$ is forward invariant and pre-asymptotically stable close to the orbit $\bar{\mathcal{O}}$ for the closed-loop system. This property descends from the fact that we use an input-output linearizing feedback to stabilize the constraint manifold, and the proof of stability is carried out via a Lyapunov analysis using Theorem 2.4. Second, we show that the target orbit $\bar{\mathcal{O}}$ is pre-asymptotically stable relative to $\bar{\Gamma}$. The key ingredient here is the computation and linearization of a Poincaré map associated with the Poincaré section P_{osc} defined in Section VII, leading to the discrete-time system (31) as discussed in Section VI. Finally, using the reduction theorem, Theorem 2.3, we deduce that the target orbit $\bar{\mathcal{O}}$ is pre-asymptotically stable for the closed-loop system, and using properties of the closed-loop system we argue that $\bar{\mathcal{O}}$ is in fact asymptotically stable, and in a neighborhood of $\bar{\mathcal{O}}$ there are no Zeno solutions.

Since for oscillations we have that $\theta^\star(q)$ is confined to a strict subset of Θ, we will assume without loss of generality that $\Theta = \mathbb{R}$.

Part 1. We start by constructing a Lyapunov function. Let

$$A \coloneqq \begin{bmatrix} 0_{n-1} & I_{n-1} \\ -K_p & -K_d \end{bmatrix}, \tag{42}$$

where $K_p, K_d \in \mathbb{R}^{(n-1)\times(n-1)}$ are the controller matrix gains in the input-output linearizing feedback $\tau^a(q,\dot{q})$ in (23), by construction independent of a. Let $P \in \mathbb{R}^{(2n-2)\times(2n-2)}$ be the symmetric positive definite solution of the Lyapunov equation $A^\top P + PA = -Q$ for some symmetric positive definite matrix $Q \in \mathbb{R}^{(2n-2)\times(2n-2)}$, consider the Lyapunov function candidate

$$W(q,\dot{q},a) \coloneqq H^\top P H. \tag{43}$$

where

$$H(q,\dot{q},a) = \begin{bmatrix} h^a(q) \\ L_{F_{\text{cl}}} h^a(q,\dot{q}) \end{bmatrix}. \tag{44}$$

This function is continuous in all of $T\mathcal{Q}\times\mathsf{A}$ and enjoys the following properties:

$$(\forall (q,\dot{q},a) \in \mathsf{C})\ L_{F_{\text{cl}}} W = -H^\top Q H \tag{45}$$

$$(\forall (q,\dot{q},a) \in \mathsf{D})\ W \circ G_{\text{cl}} - W = 0. \tag{46}$$

Property (45) is a direct consequence of our construction and the fact that $L^2_{F_{\text{cl}}} h^a = -K_p h^a - K_d L_{F_{\text{cl}}} h^a$ and therefore $L_{F_{\text{cl}}} H = AH$.

For property (46), consider the case where $(q,\dot{q},a) \in \mathsf{D}$ and $\mathsf{d} = 1$. From the definition of D we have that $|\theta^\star(q) - \vartheta| \geq \delta$ and from the geometric property (18b) we have that $\phi^a(\theta^\star(q)) = 0$ and $(\partial_\theta \phi^a)_{\theta=\theta^\star(q)} = 0$. Using the definition of h^a in (14) we have that $h^a(q) = h(q)$ and $L_{F_{\text{cl}}} h^a(q) = (dh)_q \dot{q}$. From the jump map G_{cl} in (25) we have that $\mathsf{d}^+ = -1$ and $\vartheta^+ = \theta^\star(q)$, while $q, \dot{q}$ remain unchanged. From the geometric property (19a) we have that $\phi^{a^+}(\theta^\star(q)) = 0$ and from (17b) we have that $(\partial_\theta \phi^{a^+})_{\theta=\theta^\star(q)} = 0$. Using the definition of h^a in (25) again we have that $h^{a^+}(q) = h(q)$ and $L_{F_{\text{cl}}} h^{a^+}(q) = (dh)_q \dot{q}$, and therefore $H \circ G_{\text{cl}}(q,\dot{q},a) = H(q,\dot{q},a)$. Since the matrix P in (43) is independent of a, the latter identity implies that $W \circ G_{\text{cl}}(q,\dot{q},a) - W(q,\dot{q},a) = 0$. The argument for the case where $\mathsf{d} = -1$ is entirely analogous.

Next, we note that

$$W^{-1}(0) = \{(q,\dot{q},a) \mid h^a(q) = 0,\ (\partial_q h^a)_q \dot{q} = 0\}. \tag{47}$$

From the definition of the hybrid constraint manifold $\bar{\Gamma}$ in (13) we note that

$$W^{-1}(0) \cap \mathsf{C} = \bar{\Gamma}. \tag{48}$$

Since 0 is a global minimum of W then properties (45) and (48) imply that any solution starting on $\bar{\Gamma}$ stays in $\bar{\Gamma}$ during flow. Furthermore, since we also have that $G_{\text{cl}}(\mathsf{D}) \subset \mathsf{C}$ then properties (46) and (48) imply that any solution starting on $\bar{\Gamma}$ remains on $\bar{\Gamma}$ during jumps. Therefore, we have that the set $\bar{\Gamma}$ is forward invariant. This proves part (a) of Theorem 6.1.

Finally, we want to show that $\bar{\Gamma}$ is pre-asymptotically stable close to the lifted orbit $\bar{\mathcal{O}}$ in the following sense: given a compact set K containing $\bar{\mathcal{O}}$ in its interior we want to show

that $\bar{\Gamma} \cap \mathsf{K}$ is pre-asymptotically stable for the restriction $\mathcal{H}_{\text{cl}}|_{\mathsf{K}}$. We will prove this using Theorem 2.4.

Since $G_{\text{cl}}(\mathsf{D}) \subset \mathsf{C}$, properties (46) and (48) imply that if $W^{-1}(0) \cap \mathsf{K}$ is pre-asymptotically stable, then $\bar{\Gamma} \cap \mathsf{K}$ is also pre-asymptotically stable. We have already shown that the function W in (43) satisfies the first three conditions of Theorem 2.4. For condition (iv) note that any solution $x(t,j)$ of $\mathcal{H}_{\text{cl}}$ satisfying $W(x(t,j)) = W(x(0,0)) > 0$ must be purely discrete since $L_{F_{\text{cl}}} W < 0$ outside of $\bar{\Gamma}$, and any flow would cause $W(x(t,j))$ to decrease. However, as discussed in Section VII, the controller $\mathcal{H}_{\text{osc}}$ does not allow consecutive jumps without an intermediate flow, and therefore there no discrete solutions. Then Theorem 2.4 implies that $\bar{\Gamma} \cap \mathsf{K}$ is pre-asymptotically stable for $\mathcal{H}_{\text{cl}}|_{\mathsf{K}}$.

Part 2.

We claim that $\bar{\mathcal{O}}$ is pre-asymptotically stable relative to $\bar{\Gamma}$ for the closed-loop system $\mathcal{H}_{\text{cl}}$.

We have shown that $\bar{\Gamma}$ is forward invariant for $\mathcal{H}_{\text{cl}}$. In order to investigate the closed-loop dynamics on $\bar{\Gamma}$, we use the diffeomorphism $R^a : T\Theta \to \Gamma^a$ given in (20) to get a global parametrization of the set $\bar{\Gamma}$ via the map $\tilde{R} : \mathbb{R} \times \mathbb{R} \times \mathsf{A} \to \bar{\Gamma}$ as $(\theta, \dot{\theta}, a) \mapsto (R^a(\theta, \dot{\theta}), a)$. We let $\tilde{\mathcal{O}} \coloneqq \tilde{R}^{-1}(\bar{\mathcal{O}})$ be the representation of the lifted orbit $\bar{\mathcal{O}}$ in $(\theta, \dot{\theta}, a)$ coordinates, and we use the map $\tilde{R}$ to define a reduced order hybrid system $\tilde{\mathcal{H}} = (\tilde{\mathsf{C}}, \tilde{F}, \tilde{\mathsf{D}}, \tilde{G})$ representing the dynamics of $\mathcal{H}_{\text{cl}}$ on $\bar{\Gamma}$, where

$$\begin{aligned} \tilde{\mathsf{C}} &= \{(\theta, \dot{\theta}, a) \mid \mathsf{d}\,\dot{\theta} \geq 0\} \cup \{(\theta, \dot{\theta}, a) \mid |\theta - \vartheta| \leq \delta\} \\ \tilde{\mathsf{D}} &= \{(\theta, \dot{\theta}, a) \mid \mathsf{d}\,\dot{\theta} = 0\} \cup \{(\theta, \dot{\theta}, a) \mid |\theta - \vartheta| = \delta\} \end{aligned} \tag{49}$$

and

$$\tilde{F}(\theta, \dot{\theta}, a) \coloneqq (\dot{\theta}, f^a(\theta, \dot{\theta}), 0) \tag{50}$$

with f^a the vector field of the reduced dynamics in (21). The jump map is

$$\tilde{G} : \begin{cases} (\theta, \dot{\theta})^+ = (\theta, \dot{\theta}) \\ (\mathsf{d}, \vartheta)^+ = (-\mathsf{d}, \theta) \\ \lambda^+ = \begin{cases} \text{sat}_{\mathsf{B}_r}(v(\theta - \theta_-)) & \mathsf{d} = 1 \\ \lambda & \mathsf{d} = -1. \end{cases} \end{cases} \tag{51}$$

In what follows, we denote by $x \coloneqq (\theta, \dot{\theta}, a)$ the state of $\tilde{\mathcal{H}}$. We also define $x_- \coloneqq (\theta_-, 0, (1, \theta_+, 0))$ and $x_+ \coloneqq (\theta_+, 0, (-1, \theta_-, 0))$, so that $\tilde{R}(x_-), \tilde{R}(x_+) \in \tilde{\mathcal{O}}$.

The relationship between $\tilde{\mathcal{H}}$ and $\mathcal{H}_{\text{cl}}$ is that every solution of $\mathcal{H}_{\text{cl}}$ initialized in $\bar{\Gamma}$ has the form $(q(t,j), \dot{q}(t,j), a(t,j)) = \tilde{R}(x(t,j))$, where $x(t,j)$ is a solution of $\tilde{\mathcal{H}}$. In particular, for such a solution, we have $(\theta^\star(q), \dot{\theta}^\star(q, \dot{q})) = (\theta, \dot{\theta})$ (where we have dropped the argument (t,j) for convenience). This follows from identity (22) (which is applicable because the set C is contained in $T\mathcal{W}$ by its definition) and the fact that $(q, \dot{q}) = R^a(\theta, \dot{\theta})$. The identity $\theta^\star(q) = \theta$ for solutions justifies using θ in place of $\theta^\star$ in the jump map and jump set, while the identity $\dot{\theta}^\star(q, \dot{q}) = \dot{\theta}$ justifies using $\dot{\theta}$ in the flow set. Finally, $\bar{\mathcal{O}}$ is pre-asymptotically stable relative to $\bar{\Gamma}$ for $\mathcal{H}_{\text{cl}}$ if $\tilde{\mathcal{O}} = \tilde{R}^{-1}(\bar{\mathcal{O}})$ is pre-asymptotically stable for $\tilde{\mathcal{H}}$. We will prove this latter property using a Poincaré-type argument.

Let $\tilde{\mathsf{P}}_{\text{osc}} \coloneqq \{(\theta, \dot{\theta}, a) : \mathsf{d} = 1, \dot{\theta} = 0\}$ be the representation in x coordinates of the Poincaré section P_{osc} defined in (33). Associated with $\tilde{\mathsf{P}}_{\text{osc}}$ there is a neighborhood $\mathsf{W}_{\text{osc}} \subset \tilde{\mathsf{P}}_{\text{osc}}$ of x_- in the relative topology, and a Poincaré return map $\mathsf{g}_{\text{osc}} : \mathsf{W}_{\text{osc}} \to \tilde{\mathsf{P}}_{\text{osc}}$ such that for each $x_0 \in \mathsf{W}_{\text{osc}}$ and each solution x of $\tilde{\mathcal{H}}$ with initial condition $x(0,0) = x_0$ there exists a nonzero $(\bar{t}, \bar{j}) \in \operatorname{dom} x$ such that:

(a) $x(\bar{t}, \bar{j}) \in \tilde{\mathsf{P}}_{\text{osc}}$,

(b) for each $(t,j) \in \operatorname{dom} x$ satisfying $0 < t + j < \bar{t} + \bar{j}$ we have $x(t,j) \notin \tilde{\mathsf{P}}_{\text{osc}}$, and

(c) $x(\bar{t}, \bar{j}) = \mathsf{g}_{\text{osc}}(x_0)$.

To see that this is the case, note that since $x_- \in \tilde{\mathsf{D}}$, the solution of $\tilde{\mathcal{H}}$ through x_- is forced to jump once, then flows. The initial jump gives $x_-^+ = (\theta_-, 0, (-1, \theta_-, 0))$, where we assume $v(0) = 0$ by the choice of feedback described in Section VI. By the geometric property (17a) in Definition 5.2, the fact that $\lambda = 0$ in x_-^+ implies that the VHC instantiated by the hybrid controller coincides with the nominal VHC, and therefore the flow map $\tilde{F}$ is the vector field of the nominal reduced dynamics in (6). This fact implies that the flow from x_-^+ brings the solution to the jump set $\tilde{\mathsf{D}}$, at the point x_+. The continuity of the jump map and the smoothness of the flow map $\tilde{F}$ ensure the existence of a neighborhood (in the relative topology) $\mathsf{W}_{\text{osc}} \subset \tilde{\mathsf{P}}_{\text{osc}}$ of x_- such that all solutions in W_{osc} reach $\tilde{\mathsf{D}}$ in finite time. The solution of $\tilde{\mathcal{H}}$ initialized at $x_+ \in \tilde{\mathsf{D}}$ jumps once, then flows. The jump gives $x_+^+ = (\theta_+, 0, (1, \theta_+, 0))$ (the jump does not alter the value of λ, which remains equal to zero). The ensuing flow then brings the solution to $x_- \in \tilde{\mathsf{P}}_{\text{osc}}$. By the smoothness of $\tilde{F}$, all solutions of $\tilde{\mathcal{H}}$ starting in $\tilde{\mathsf{D}}$ sufficiently close to x_+ will reach $\tilde{\mathsf{P}}_{\text{osc}}$. Therefore, by making if necessary W_{osc} smaller, we ensure that all solutions of $\tilde{\mathcal{H}}$ initialized in W_{osc} reach $\tilde{\mathsf{P}}_{\text{osc}}$. This establishes the existence of a well-defined Poincaré return map $\mathsf{g}_{\text{osc}} : \mathsf{W}_{\text{osc}} \to \tilde{\mathsf{P}}_{\text{osc}}$.

All solutions of $\tilde{\mathcal{H}}$ initialized in W_{osc} undergo the four phases in this diagram:

$$\begin{array}{c} (\theta, 0, (1, \vartheta, \lambda)) \in \tilde{\mathsf{D}} \; - - \overset{\tilde{G}}{-} \succ (\theta, 0, (-1, \theta, \lambda^1)) \in \tilde{\mathsf{C}} \\ \searrow^{\tilde{\mathsf{P}}_+} \\ (\theta^1, 0, (-1, \theta, \lambda^1)) \in \tilde{\mathsf{D}} \; - - \overset{\tilde{G}}{-} \succ (\theta^1, 0, (1, \theta^1, \lambda^1)) \in \tilde{\mathsf{C}} \\ \searrow^{\tilde{\mathsf{P}}_-} \\ (\theta^2, 0, (1, \theta^1, \lambda^1)) \in \tilde{\mathsf{P}}_{\text{osc}}, \end{array} \tag{52}$$

and g_{osc} maps $(\theta, 0, (1, \vartheta, \lambda))$ to $(\theta^2, 0, (1, \theta^1, \lambda^1))$, where $\lambda^1 = \text{sat}_{\mathsf{B}_r}(v(\theta - \theta_-))$. Since the action of g_{osc} is entirely characterized by the variables $(\theta, \vartheta, \lambda)$, defining a state $\tilde{z} \coloneqq [\theta \ \vartheta \ \lambda]^\top$ we consider the update law

$$\Sigma : \tilde{z} = [\theta \ \vartheta \ \lambda]^\top \mapsto \tilde{z}^+ = [\theta^2 \ \theta^1 \ v]^\top, \tag{53}$$

described by the diagram in (52). As described earlier, $\mathsf{g}_{\text{osc}}(x_-) = x_-$, so the point $\tilde{z}_- \coloneqq [\theta_- \ \theta_+ \ 0]^\top$ is a fixed point of Σ corresponding to the control input $v = 0$. We drop the dependency of v on θ and regard v as a control input.

We seek to find the linearization of Σ at the fixed point $\tilde{z}_-$ corresponding to $v = 0$. This linearization has the form $\delta\tilde{z}^+ = A\,\delta\tilde{z} + Bv$, where $A = \partial_{\tilde{z}} \Sigma\big|_{\tilde{z} = \tilde{z}_-, v = 0}$, $B = \partial_v \Sigma\big|_{\tilde{z} = \tilde{z}_-, v = 0}$, and $\delta\tilde{z} \coloneqq \tilde{z} - \tilde{z}_-$.

In order to compute these Jacobians, we need to determine the partial derivatives of θ^1, θ^2 with respect to $\theta, \vartheta, \lambda$ and v, and for that we recall that during each one of the two flows in (52), the orbits of the flow map preserve the energy function $E^a = (1/2)M^a(\theta)\dot{\theta}^2 + V^a(\theta)$, for the value of a associated with the given phase. In the following computations we will replace λ^1 by v since for small enough v we have that $\mathrm{sat}_{\mathsf{B}_r}(v) = v$.

To compute $(\partial_{\tilde{z}}\theta^1)|_{\tilde{z}_-}$, we consider the solution starting at $(\theta, 0, (-1, \theta, v))$ and ending at $(\theta^1, 0, (-1, \theta, v))$, and note that said solution starts and ends with $\dot{\theta} = 0$, so θ^1 is described implicitly by the requirement that the virtual potential $V^a(\theta)$ be equal at the beginning and end of the flow: $V^a(\theta) = V^a(\theta^1)$, with $a = (-1, \theta, v)$. An analogous consideration holds for the second flow so θ^1 and θ^2 are implicitly defined by the identities

$$\eta^+(\theta, \theta^1, v) \coloneqq V^{(-1,\theta,v)}(\theta^1) - V^{(-1,\theta,v)}(\theta) = 0 \tag{54a}$$

$$\eta^-(\theta^1, \theta^2, v) \coloneqq V^{(1,\theta^1,v)}(\theta^2) - V^{(1,\theta^1,v)}(\theta^1) = 0. \tag{54b}$$

Since $\theta^1|_{\tilde{z}=\tilde{z}_-} = \theta_+$ and using the geometric property (17a), we have

$$\begin{aligned}\partial_{\theta^1}\eta^+(\theta, \theta^1, v)\big|_{(\theta_-,\theta_+,0)} &= \partial_\theta V^{(-1,\theta_-,0)}(\theta)\big|_{\theta=\theta_+} \\ &= \partial_\theta V|_{\theta=\theta_+},\end{aligned}$$

where V is the nominal virtual potential in (8). Noting that $\partial_\theta V_\theta = -\Psi_1(\theta)M(\theta)$, and that $M(\theta) > 0$, we see that $\partial_\theta V|_{\theta=\theta_+} \neq 0$ because, by definition of θ_+ on (10), $\Psi_1(\theta_+) > 0$. Therefore, $\partial_{\theta^1}\eta^+(\theta, \theta^1, v)\big|_{(\theta_-,\theta_+,0)} \neq 0$. In the same manner we establish that $\partial_{\theta^2}\eta^-(\theta^1, \theta^2, v)\big|_{(\theta_+,\theta_-,0)} \neq 0$. Applying the implicit function theorem to (54a) and using the geometric property (17a), we get

$$\begin{aligned}\partial_\theta\theta^1\big|_{(\tilde{z}_-,0)} &= -\left(\partial_\theta\eta^+/\partial_{\theta^1}\eta^+\right)\big|_{(\theta_-,\theta_+,0)} \\ &= (\partial_\theta V|_{\theta_-})/(\partial_\theta V|_{\theta_+}) \\ \partial_\vartheta\theta^1\big|_{(\tilde{z}_-,0)} &= 0 \\ \partial_\lambda\theta^1\big|_{(\tilde{z}_-,0)} &= 0 \\ \partial_v\theta^1\big|_{(\tilde{z}_-,0)} &= -\left(\partial_v\eta^+/\partial_{\theta^1}\eta^+\right)\big|_{(\theta_-,\theta_+,0)} \\ &= \frac{\partial_\lambda|_{\lambda=0}\left(V^{(-1,\theta_-,\lambda)}(\theta_-) - V^{(-1,\theta_-,\lambda)}(\theta_+)\right)}{\partial_\theta V|_{\theta_+}}.\end{aligned} \tag{55}$$

In a similar manner, applying now the implicit function theorem to the identity (54b) and using the geometric property (17a) and the chain rule we obtain

$$\begin{aligned}\partial_\theta\theta^2\big|_{(\tilde{z}_-,0)} &= -\left(\partial_{\theta^1}\eta^-/\partial_{\theta^2}\eta^-\right)\big|_{(\theta_+,\theta_-,0)}\partial_\theta\theta^1\big|_{(\tilde{z}_-,0)} = 1 \\ \partial_\vartheta\theta^2\big|_{(\tilde{z}_-,0)} &= 0 \\ \partial_\lambda\theta^2\big|_{(\tilde{z}_-,0)} &= 0 \\ \partial_v\theta^2\big|_{(\tilde{z}_-,0)} &= -\left(\partial_v\eta^-/\partial_{\theta^2}\eta^-\right)\big|_{(\theta_+,\theta_-,0)} \\ &\quad -\left(\partial_{\theta^1}\eta^-/\partial_{\theta^2}\eta^-\right)\big|_{(\theta_+,\theta_-,0)}\partial_v\theta^1\big|_{(\tilde{z}_-,0)} \\ &= b/(\Psi_1(\theta_-)M(\theta_-)),\end{aligned} \tag{56}$$

where b is the constant vector defined in (32) and we use the fact that $\partial_\theta V|_{\theta_-} = -\Psi_1(\theta_-)M(\theta_-)$. Using these partials and the expression for the map Σ in (53) we arrive at the following linearized system at $\tilde{z}_-$:

$$\delta\tilde{z}^+ = \begin{bmatrix} 1 & 0 & 0 \\ A_{21} & 0 & 0 \\ 0 & 0 & 0 \end{bmatrix}\delta\tilde{z} + \begin{bmatrix} b/(\Psi_1(\theta_-)M(\theta_-)) \\ B_2 \\ 1 \end{bmatrix} v, \tag{57}$$

where A_{21}, B_2 are the respective partials in (55). The above linearization is stabilizable because, by assumption, $b \neq 0$. Its controllable subsystem is given by the first state, and it coincides with system (31). By construction, the discrete-time feedback v asymptotically stabilizes the origin of (31), and thus it also asymptotically stabilizes the origin of (57). We conclude that the hybrid controller $\mathcal{H}_{\text{osc}}$ in Theorem 6.1 renders the fixed point $\tilde{z}_-$ asymptotically stable for Σ, which in turn implies that x_- is an asymptotically stable fixed point of g_{osc}.

Asymptotic stability of $\tilde{z}_-$ for Σ implies existence of a closed neighborhood $\mathsf{U} \subset \mathsf{W}_{\text{osc}}$ of x_- and of a Lyapunov function $W : \mathsf{U} \to \mathbb{R}$ that is positive definite with respect to x_- and such that $\Delta W = W \circ \mathsf{g}_{\text{osc}} - W$ is negative definite with respect to x_- on U. Next, we will extend W, defined on a subset of the Poincaré section P_{osc}, to construct a Lyapunov function $\tilde{W}$ defined in a neighborhood of $\tilde{\mathcal{O}}$. Using the maps defined in the diagram (52) we construct a retraction onto U,

$$Z(x) = \begin{cases} \tilde{\mathsf{P}}_-(x) & \text{if } \mathsf{d} = 1 \\ \tilde{\mathsf{P}}_- \circ \tilde{G} \circ \tilde{\mathsf{P}}_+(x) & \text{if } \mathsf{d} = -1. \end{cases} \tag{58}$$

For any point $x \in \operatorname{dom} Z$, the map Z gives us the first point at which the solution starting from x intersects P_{osc}. We take $\tilde{\mathsf{U}} = \operatorname{dom} Z = Z^{-1}(\mathsf{U})$. Since Z is a composition of continuous maps it is also continuous. We note that $Z^{-1}(x_-) = \tilde{\mathcal{O}}$, and since U is a closed neighborhood of x_-, we have that $\tilde{\mathsf{U}}$ is a closed neighborhood of $\tilde{\mathcal{O}}$. We already know that this map does not change during flow. Furthermore, for any jumps where $\mathsf{d} = 1$ we have that $Z \circ \tilde{G}(x) = \mathsf{g}_{\text{rot}}(x)$, and for any jumps where $\mathsf{d} = -1$ we have $Z \circ \tilde{G}(x) = Z(x)$.

Taking $\tilde{W} = W \circ Z$, we have $L_{\tilde{F}}\tilde{W} = 0$ during flow, $\Delta\tilde{W} = 0$ when $x \in \tilde{\mathsf{D}}$ and $\mathsf{d} = -1$, and $\Delta\tilde{W} = W \circ \mathsf{g}_{\text{rot}} - W < 0$ when $x \in \tilde{\mathsf{D}} \setminus \{x_-\}$ and $\mathsf{d} = 1$. Therefore $\tilde{W}$ satisfies conditions (i), (ii) and (iii) of Theorem 2.4. For condition (iv), we note that any solution $x(t, j)$ of $\tilde{\mathcal{H}}$ satisfying $\tilde{W}(x(t, j)) = \tilde{W}(x(0, 0)) > 0$ must not have any jumps on $\tilde{\mathsf{D}}$ with $\mathsf{d} = 1$, since any such jump would cause $\tilde{W}(x(t, j))$ to decrease. However, we know from the definition of $\tilde{\mathsf{U}}$ that any complete solution starting on $\tilde{\mathsf{U}}$ will eventually reach $\mathsf{U} \subset \mathsf{P}_{\text{rot}}$ where $\mathsf{d} = 1$ and jump, and therefore Condition (iv) is satisfied.

Since all conditions of Theorem 2.4 are satisfied for $\tilde{\mathcal{H}}|_{\tilde{\mathsf{U}}}$ using $\tilde{W}$, we see that $\tilde{\mathcal{O}}$ is pre-asymptotically stable for $\tilde{\mathcal{H}}|_{\tilde{\mathsf{U}}}$ and using Lemma 2.2 with $\Gamma_1 = \tilde{\mathcal{O}}$ and $\Gamma_2 = \tilde{\mathsf{U}}$, we conclude that $\tilde{\mathcal{O}}$ is pre-asymptotically stable for $\tilde{\mathcal{H}}$ and therefore $\bar{\mathcal{O}}$ is pre-asymptotically stable relative to $\bar{\Gamma}$.

Part 3. We have shown that $\bar{\Gamma} \cap \mathsf{K}$ is pre-asymptotically stable for $\mathcal{H}_{\text{cl}}|_{\mathsf{K}}$, and that $\bar{\mathcal{O}}$ is pre-asymptotically stable relative to $\bar{\Gamma}$ for $\mathcal{H}_{\text{cl}}$. This latter fact implies that $\bar{\mathcal{O}}$ is pre-asymptotically stable relative to $\bar{\Gamma} \cap \mathsf{K}$ for $\mathcal{H}_{\text{cl}}|_{\mathsf{K}}$. By Theorem 2.3, $\bar{\mathcal{O}}$ is pre-asymptotically stable for $\mathcal{H}_{\text{cl}}|_{\mathsf{K}}$. Furthermore, since K is closed

and contains $\bar{\mathcal{O}}$ in its interior, Lemma 2.2 implies that $\bar{\mathcal{O}}$ is pre-asymptotically stable for $\mathcal{H}_{\text{cl}}$.

Stability of $\bar{\mathcal{O}}$ implies the existence of a compact forward invariant neighborhood U of $\bar{\mathcal{O}}$. Since $\mathcal{O}$ is in the interior of $T\mathcal{W} \times \mathsf{A}$, we can assume that U is in the interior of $T\mathcal{W} \times \mathsf{A}$ as well. As discussed in Section VII, maximal solutions of $\mathcal{H}_{\text{cl}}$ can only terminate if the state $(q, \dot{q})$ would move outside of $T\mathcal{W}$ during flow. Since solutions that stay in U cannot leave $T\mathcal{W}$, they must be complete, and therefore $\bar{\mathcal{O}}$ is asymptotically stable.

Finally, since U is compact, then $\dot{\theta}^\star(q, \dot{q})$ is bounded for solutions starting on U. Since we have that $|\theta^\star(q) - \vartheta| \geq \delta$ on D and $\vartheta = \theta^\star(q)$ after jumps, the fact that $\dot{\theta}^\star(q, \dot{q})$ is bounded implies that there is a minimum time between jumps and therefore there are no Zeno solutions starting on U. This concludes the proof of Theorem 6.1. ■

Remark 11.1: The proof of Theorem 6.1 shares similarities with the orbital stability proof in [24, Corollary 11] (see also [14, Theorem 16]), and more broadly with the orbital stability proofs found in the book [33] and related papers such as [34]. At the core of all these proofs there is a Poincaré analysis, and some argument aiming to reduce the dimensionality of the stability analysis by restricting it to the constraint manifold. In [33], [24] the dimensionality reduction is achieved either through finite-time stabilization of the constraint manifold or through fast stabilization using high-gain control. In this paper, the dimensionality reduction is achieved through the hybrid reduction theorem (Theorem 2.3) which requires neither finite-time stabilization nor high-gain control.

A further theoretical challenge lies in the fact that once one establishes that the equilibrium on a Poincaré section is asymptotically stable for the associated Poincaré map, one must in some way deduce that the closed orbit corresponding to said equilibrium is orbitally stable. In the context of hybrid systems, this deduction is non-trivial and requires a dedicated analysis, which is what we do in part 2 of our proof using the retraction $Z : \tilde{U} \to U$.

Finally, there are differences between our proof and the ones in the literature due to the differences in the class of systems and the control goal, as discussed in the introduction. △

XII. Conclusion

We have presented a hybrid controller stabilizing target oscillations for mechanical control systems with degree of underactuation one. The controller is hierarchical, with a low-level continuous controller enforcing a VHC in a family, and a high-level hybrid supervisor selecting the VHC in the family. The main stability theorem asserts local asymptotic stability of the target orbit. Since the stabilization mechanism relies on the discrete-event updates to the VHC parameters, there are limitations on the possible basin of attraction based on the energy level of the initial condition. If the initial energy is too high, the resulting solution may never change the direction of movement, and if the initial energy is too low then $\theta^\star(q)$ may remain within a δ neighborhood of the initial condition. In both cases, the jump set is never reached and the controller cannot drive the state close to the desired orbit. In future work we will investigate adding a further layer in the control hierarchy to ensure asymptotic stabilization with a *guaranteed* basin of attraction. The control technique presented in this paper can be adapted to stabilizing rotations, and this will be the subject of future work.

References

[1] C. I. Byrnes and A. Isidori, "Asymptotic stabilization of minimum phase nonlinear systems," *IEEE Transactions on Automatic Control*, vol. 36, no. 10, pp. 1122–1137, 1991.

[2] C. Canudas-de Wit, B. Espiau, and C. Urrea, "Orbital stabilization of underactuated mechanical systems," *IFAC Proceedings Volumes*, vol. 35, no. 1, pp. 527–532, 2002.

[3] L. Consolini and M. Maggiore, "On the swing-up of the pendubot using virtual holonomic constrains," *IFAC Proceedings Volumes*, vol. 44, no. 1, pp. 9290–9295, 2011.

[4] ——, "Control of a bicycle using virtual holonomic constraints," *Automatica*, vol. 49, no. 9, pp. 2831–2839, 2013.

[5] ——, "Synthesis of virtual holonomic constraints for 3-dof mechanical systems," in *52nd IEEE Conference on Decision and Control*. IEEE, 2013, pp. 2888–2893.

[6] L. Consolini, M. Maggiore, C. Nielsen, and M. Tosques, "Path following for the pvtol aircraft," *Automatica*, vol. 46, no. 8, pp. 1284–1296, 2010.

[7] A. Costalunga and L. Consolini, "Synthesis of virtual holonomic constraints for obtaining stable constraint dynamics," *Automatica*, vol. 93, pp. 262–273, 2018.

[8] L. Freidovich, A. Robertsson, A. Shiriaev, and R. Johansson, "Periodic motions of the pendubot via virtual holonomic constraints: Theory and experiments," *Automatica*, vol. 44, no. 3, pp. 785–791, 2008.

[9] L. Freidovich, A. Shiriaev, and I. Manchester, "Transitions between limit cycles for an underactuated system: Virtual constraints approach," *IFAC Proceedings Volumes*, vol. 40, no. 12, pp. 468–473, 2007.

[10] T. Fukuda, S. Kojima, K. Sekiyama, and Y. Hasegawa, "Design method of brachitation controller based on virtual holonomic constraint," in *2007 IEEE/ASME international conference on advanced intelligent mechatronics*. IEEE, 2007, pp. 1–6.

[11] T. Fukuda and F. Saito, "Motion control of a brachiation robot," *Robotics and autonomous systems*, vol. 18, no. 1-2, pp. 83–93, 1996.

[12] R. Goebel, R. G. Sanfelice, and A. R. Teel, *Hybrid dynamical systems*. Princeton University Press, 2012.

[13] M. W. Gomes and A. L. Ruina, "A five-link 2d brachiating ape model with life-like zero-energy-cost motions," *Journal of theoretical biology*, vol. 237, no. 3, pp. 265–278, 2005.

[14] J. W. Grizzle, C. Chevallereau, R. W. Sinnet, and A. D. Ames, "Models, feedback control, and open problems of 3d bipedal robotic walking," *Automatica*, vol. 50, no. 8, pp. 1955–1988, 2014.

[15] V. Guillemin and A. Pollack, *Differential Topology.* New Jersey: Prentice Hall, 1974.

[16] J. Hauser and R. Hindman, "Maneuver regulation from trajectory tracking: Feedback linearizable systems," *IFAC Proceedings Volumes*, vol. 28, no. 14, pp. 595–600, 1995.

[17] A. Isidori, *Nonlinear Control Systems, 3rd Edition*. Springer Verlag, 1995.

[18] J. M. Lee, *Introduction to Smooth Manifolds*. Springer, 2012.

[19] M. Maggiore and L. Consolini, "Virtual holonomic constraints for Euler–Lagrange systems," *IEEE Transactions on Automatic Control*, vol. 58, no. 4, pp. 1001–1008, 2013.

[20] M. Maggiore, M. Sassano, and L. Zaccarian, "Reduction theorems for hybrid dynamical systems," *IEEE Transactions on Automatic Control*, vol. 64, no. 6, pp. 2254–2265, 2019.

[21] A. Mohammadi, M. Maggiore, and L. Consolini, "On the Lagrangian structure of reduced dynamics under virtual holonomic constraints," *ESAIM: Control, Optimisation and Calculus of Variations*, vol. 23, no. 3, pp. 913–935, 2017.

[22] ——, "Dynamic virtual holonomic constraints for stabilization of closed orbits in underactuated mechanical systems," *Automatica*, vol. 94, pp. 112–124, 2018.

[23] A. Mohammadi, E. Rezapour, M. Maggiore, and K. Y. Pettersen, "Maneuvering control of planar snake robots using virtual holonomic constraints," *IEEE Transactions on Control Systems Technology*, vol. 24, no. 3, pp. 884–899, 2015.

[24] B. Morris and J. W. Grizzle, "Hybrid invariant manifolds in systems with impulse effects with application to periodic locomotion in bipedal robots," *IEEE Transactions on Automatic Control*, vol. 54, no. 8, pp. 1751–1764, 2009.

[25] J. Nakanishi, T. Fukuda, and D. E. Koditschek, "A brachiating robot controller," *IEEE Transactions on Robotics and Automation*, vol. 16, no. 2, pp. 109–123, 2000.
[26] Q. Nguyen, X. Da, J. Grizzle, and K. Sreenath, "Dynamic walking on stepping stones with gait library and control barrier functions," in *Algorithmic Foundations of Robotics XII: Proceedings of the Twelfth Workshop on the Algorithmic Foundations of Robotics*. Springer, 2020, pp. 384–399.
[27] R. Ortega, B. Yi, J. G. Romero, and A. Astolfi, "Orbital stabilization of nonlinear systems via the immersion and invariance technique," *International Journal of Robust and Nonlinear Control*, vol. 30, no. 5, pp. 1850–1871, 2020.
[28] R. Otsason and M. Maggiore, "Virtual constraint generators for motion control of robots with degree of underactuation one," *Submitted to Automatica*, 2022.
[29] ——, "On the generation of virtual holonomic constraints for mechanical systems with underactuation degree one," in *2019 IEEE 58th Conference on Decision and Control (CDC)*. IEEE, 2019, pp. 8054–8060.
[30] R. G. Sanfelice, *Hybrid Feedback Control*. Princeton University Press, 2021.
[31] A. S. Shiriaev, L. B. Freidovich, and S. V. Gusev, "Transverse linearization for controlled mechanical systems with several passive degrees of freedom," *IEEE Transactions on Automatic Control*, vol. 55, no. 4, pp. 893–906, 2010.
[32] A. Shiriaev, J. Perram, and C. Canudas-de-Wit, "Constructive tool for orbital stabilization of underactuated nonlinear systems: Virtual constraints approach," *IEEE Trans. Automat. Contr.*, vol. 50, no. 8, pp. 1164–1176, August 2005.
[33] E. Westervelt, J. Grizzle, C. Chevallereau, J. Choi, and B. Morris, *Feedback Control of Dynamic Bipedal Robot Locomotion*. Florida, United States: CRC Press, 2007.
[34] E. Westervelt, J. Grizzle, and D. Koditschek, "Hybrid zero dynamics of planar biped robots," *IEEE Transactions on Automatic Control*, vol. 48, no. 1, pp. 42–56, 2003.
[35] E. R. Westervelt, J. W. Grizzle, and C. C. De Wit, "Switching and pi control of walking motions of planar biped walkers," *IEEE Transactions on automatic control*, vol. 48, no. 2, pp. 308–312, 2003.
[36] B. Yi, R. Ortega, D. Wu, and W. Zhang, "Orbital stabilization of nonlinear systems via mexican sombrero energy shaping and pumping-and-damping injection," *Automatica*, vol. 112, p. 108661, 2020.

Luiz Navarro was born in Brasilia, Brazil. He received the Bachelors degree in Mechatronics Engineering in 2014 from the University of Brasilia and the M.Eng degree in Electric Engineering from the University of Toronto in 2019. He is currently a PhD student in the Edward S. Rogers Sr. Department of Electrical and Computer Engineering, University of Toronto, Canada. His research focuses on geometric nonlinear control.

Manfredi Maggiore was born in Genoa, Italy. He received the "Laurea" degree in Electronic Engineering in 1996 from the University of Genoa and the PhD degree in Electrical Engineering from the Ohio State University, USA, in 2000. Since 2000 he has been with the Edward S. Rogers Sr. Department of Electrical and Computer Engineering, University of Toronto, Canada, where he is currently Professor. He has been a visiting Professor at the University of Bologna (2007-2008), and the Laboratoire des Signaux et Systèmes, Ecole CentraleSupélec (2015-2016). His research focuses on mathematical nonlinear control and geometric mechanics.